Hybrid Model for Optimization Of Crude Distillation Units

By

GANG FU

A Thesis

Submitted to the school of Graduate Studies

In Partial Fulfillment of the Requirements

For the Degree

Master of Applied Science

McMaster University

2015.08

Abstract

Planning, scheduling and real time optimization (RTO) are currently implemented by using different types of models, which causes discrepancies between their results. This work presents a single model of a crude distillation unit (preflash, atmospheric, and vacuum towers) suitable for all of these applications, thereby eliminating discrepancies between models used in these decision processes. Hybrid model consists of volumetric and energy balances and partial least squares model for predicting product properties. Product TBP curves are predicted from feed TBP curve, operating conditions (flows, pumparound heat duties, furnace coil outlet temperatures). Simulated plant data and model testing have been based on a rigorous distillation model, with 0.5% RMSE over a wide range of conditions. Unlike previous works, we do not assume that (i) midpoint of a product TBP curve lies on the crude distillation curve, and (ii) midpoint between the back-end and front-end of the adjacent products lies on the crude distillation curves, since these assumptions do not hold in practice. Associated properties (e.g. gravity, sulfur) are computed for each product based on its distillation curve. Model structure makes it particularly amenable for development from plant data. High model accuracy and its linearity make it suitable for optimization of production plans or schedules.

Acknowledgements

I would like to acknowledge and gratitude to my supervisor Dr. Vladimir Mahalec, for giving me this opportunity to work in this research. Without his constant support and encouragement, it is not possible to complete this research. His kindness, patience, advice, comments and suggestions were very helpful throughout the entire research.

I would like to thank my friends Pedro, Philip, Erik, Omar, Fahal, and Smriti, who helped me during this research.

I would also like to thanks all my family, especially my wife Lei and my boy Daniel, who gives me endless love and motivation.

Table of Contents

List of Illustrations

List of Tables

Nomenclature

Abbreviations

TBP	true boiling point (F)
TBPxx	true boiling point of xx% percent distillated (liquid volume based) (F)
IBP	initial boiling point, TBP01 (F)
FBP	final boiling point, TBP99 (F)
PF	preflash tower
AP	atmospheric tower
VP	vacuum tower
STM	bottom steam
SS	stripper steam
PA	pumparound
COT	coil outlet temperature
COND	condenser
SG	specific gravity (g/cm^3)
VTR	volumetric transfer ratio
WTR	weight transfer ratio
LSM	least squares method
wt%	weight percentage
LV%	liquid volume percentage
sw-1	swing-cut 1(swing cut between heavy naphtha and kerosene)
sw-2	swing-cut 2(swing cut between kerosene and diesel)
sw-3	swing-cut 3(swing cut between diesel and ago)
sw1-l	light part swing-cut 1
sw1-h	heavy part swing-cut 1
sw2-l	light part swing –cut 2
sw2-h	heavy part swing-cut 2
sw3-l	light part swing-cut 3
sw3-h	heavy part swing-cut 3
L/H	improved swing cut light and heavy method

Subscripts

lgh	light (gas) from vapor of preflash
nph	naphtha from top of preflash
$hnph$	heavy naphtha from top of preflash
$kero$	kerosene from atmospheric tower
dsl	diesel from atmospheric tower
AGO	atmospheric gasoil from atmospheric tower
$lvgo$	light vacuum gasoil from vacuum tower
$hvgo$	heavy vacuum gasoil from vacuum tower
$resid$	residue in vacuum tower
fur	furnace
dry	not consider water in hydrocarbon mix
$water$	consider water in hydrocarbon mix
i	hydrocarbon (feed or products)
j	point on TBP curve(01,05,10,30,50,70,90,95,99)
k	pumparound
u	unit (preflash, atmospheric tower, vacuum tower)

Variables

$fraction$	fraction of crude oil in crude oil mix
F	volumetric flowrate (bbl/day)
MF	mass flowrate (lb/h)
$feed_u$	feed steam entering into unit u(bbl/day)
stm_u	botton steam in unit u(lb/h)
$water_u$	top condenser liquid water outlet in unit u(lb/h)
$top-vapor$	top vapor water outlet in vacuum tower(lb/h)
ρ_i	density of hydrocarbon i (lb/bbl)
h_i	enthalpy of hydrocarbon i in liquid phase ($mmbtu/lb$)
H_i	enthalpy of hydrocarbon i in vapor phase ($mmbtu/lb$)
h_{water}	enthalpy of in water liquid phase ($mmbtu/lb$)
H_{water}	enthalpy of water in vapor phase ($mmbtu/lb$)
$Qduty_{u,QPA_k}$	pumparound k duty in unit u ($mmbtu/h$)
$Qduty_{u,fur}$	furnace duty in unit u ($mmbtu/h$)
$Q_{cond}(wet)_u$	condenser duty in unit u in water based($mmbtu/h$)

$Q_{cond}(dry)_u$	condenser duty in unit u in dry based($mmbtu/h$)
$Q_{cond}(water)_u$	condenser duty for condensing water in unit u in dry based ($mmbtu/h$)
$C_{i,L}$	specific heat capacity of product i at constant pressure in liquid phase ($mmbtu/(lb*F)$)
$C_{i,V}$	specific heat capacity of product i at constant pressure in vapor phase ($mmbtu/(lb*F)$)
h_i^0	enthalpy of product i in liquid phase for basic case ($mmbtu/lb$)
H_i^0	enthalpy of product i in vapor phase for basic case ($mmbtu/lb$)
T_i	temperature of product i (F)
T_i^0	temperature of product i for basic case (F)
$T_{draw\_off\_tray,i}$	draw off tray temperature of product i (F)
ss_i	side stripper steam for product i in atmospheric tower (lb/h)
$y_{u,i}$	yield of product i in unit u($\%$)
λ_d	heat of vaporization of distillate of atmospheric tower($mmbtu/lb$)
λ_d^0	heat of vaporization of distillate of atmospheric tower for basic case ($mmbtu/lb$)
$TBP_{d,50}$	distillate TBP50 temperature(F)
$ccwp_{u,i}$	cumulative cut width of product i in unit u ($\%$)
$cutt_{u,i}$	cut point of product i in unit u (F)
$TBP_{i,j}$	TBP j on product i (F)
$TBP'_{i,j}$	linear extrapolate TBP j on product i on middle straight line (F)
$TBP^d_{i,j}$	vertical deviation between middle straight line and TBPj on product i (F)
φ	vapor fraction of atmospheric feed
$RefluxRatio$	reflux/(reflux + distillate) in atmospheric tower (volume based)
$\Delta TGap_{i,i+1}$	difference temperature between TBP50 of adjacent product i and $i+1$
$a_{0,1,2,3,4}$	coefficient in heat of vaporization calculation
$a_{i,j,n}$	coefficient of the TBP statistical models

1. Introduction

1.1 Crude distillation unit

Crude distillation units (CDUs) separate feed to a refinery into intermediate products which are further process by the downstream units or blended into the final products. CDUs are complex distillation towers, producing several products and having many degrees of freedom which can be used to fine-tune the operation. Fig.1 shows an example of a CDU in Aspen Plus (2006) consisting of a preflash tower (which remove light components from the feed), atmospheric distillation (which operates at atmospheric pressure and separates bulk of the crude into several products), and vacuum distillation (which operates under vacuum to separate heavy end of the crude into several products).

Since crude oil typically consist of large number of compounds, and its chemical compositions is not known, petroleum refining community has adopted crude characterization in a form of crude assays. An assay describes a crude oil in terms of increasing boiling point temperatures at which specific parts of the crude will evaporate; this is so called true boiling point (TBP) curve, as shown in Fig.2. The entire TBP curve is divided into non-overlapping sections ("cuts"). Other crude properties, e.g. % sulfur or gravity or viscosity, also vary from one temperature range to another temperature range (from one cut to another), as shown in Fig. 3 and Fig. 4.

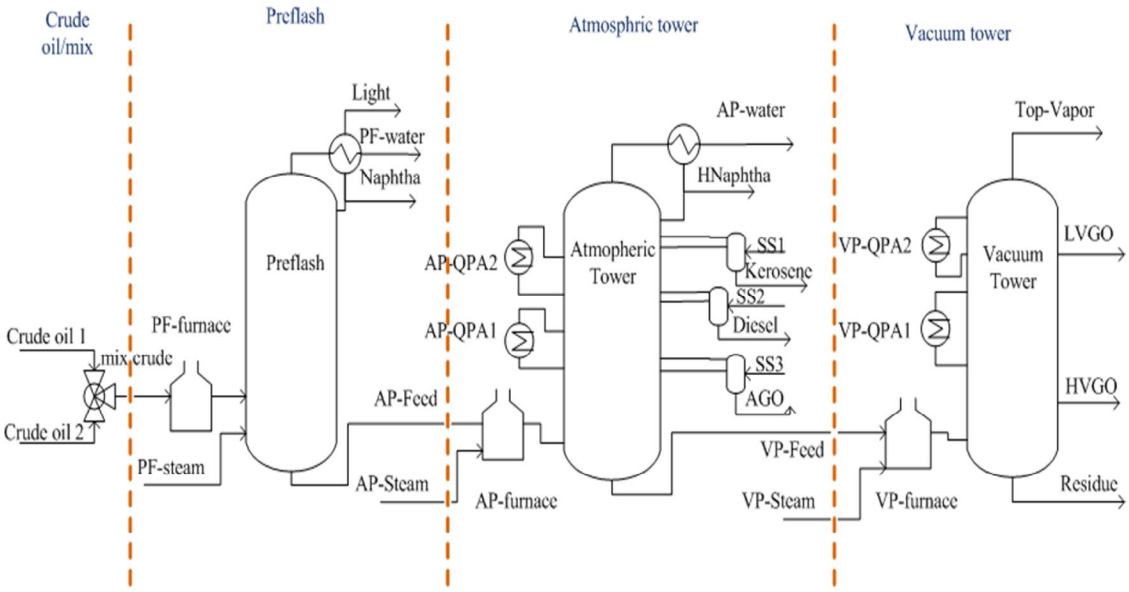

Figure 1. Crude distillation unit example

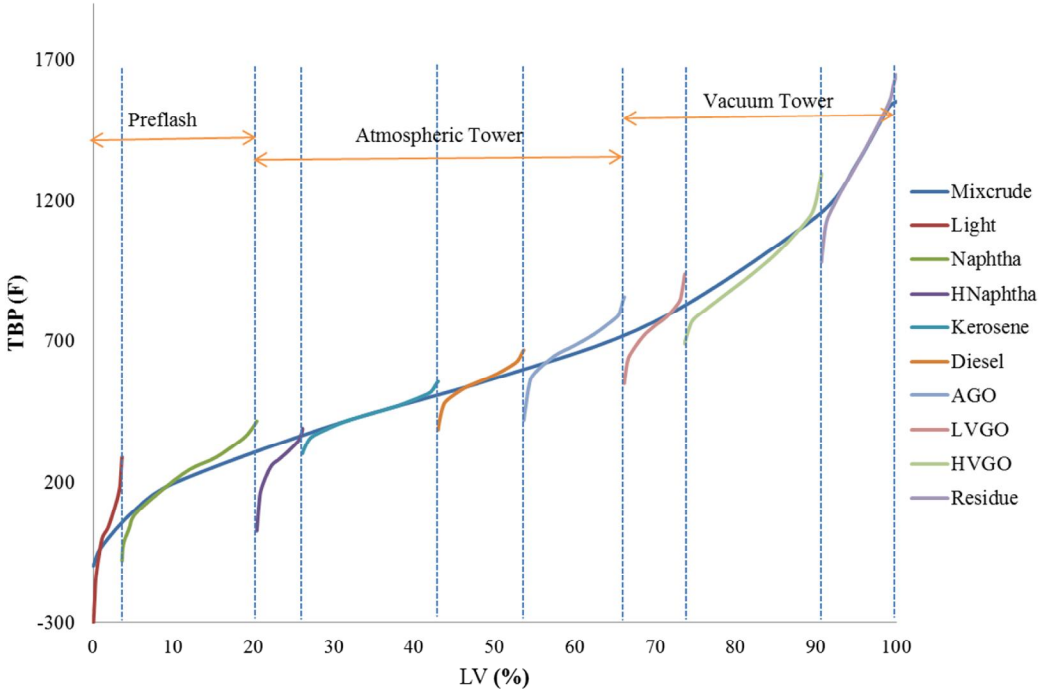

Figure 2. TBP curve for crude distillation unit

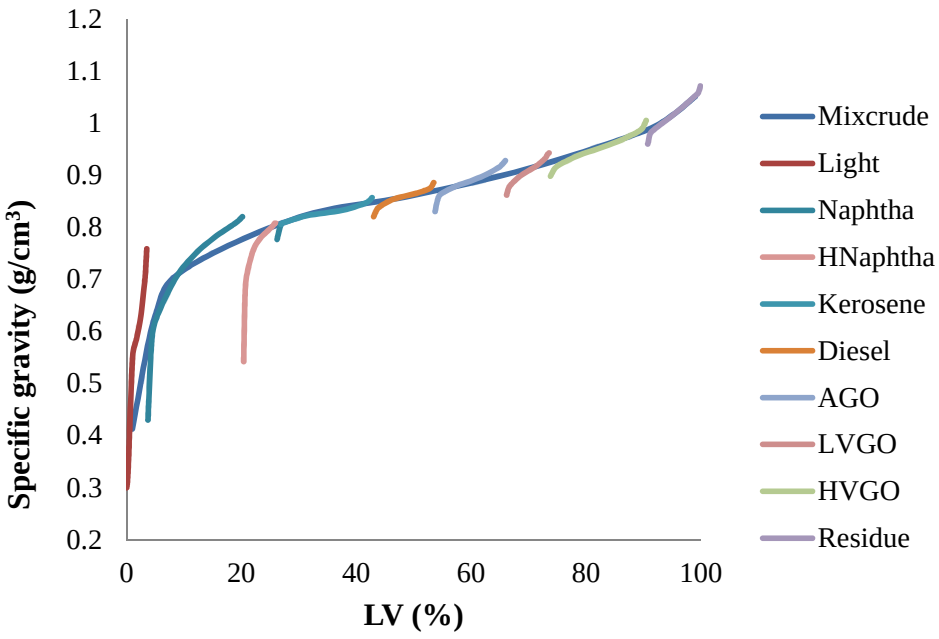

Figure 3. Specific gravity of products of CDUs

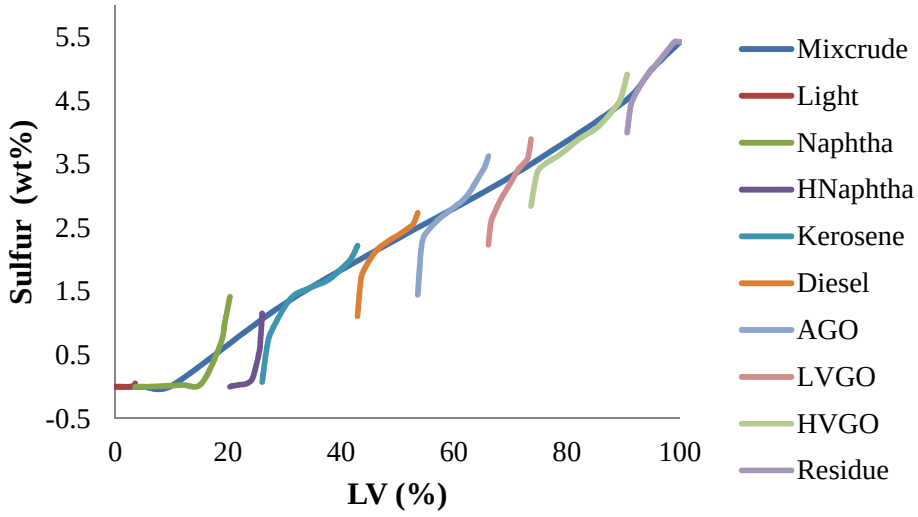

Figure 4. Sulfur content of products of CDUs

If CDU is capable of perfectly sharp separation, each product stream from CDU will have the yield corresponding to the width of the cut and its TBP curve will overlap its section of the crude TBP curve. In reality, product distillation curves differ significantly from their respective section of the crude TBP curve. Fig. 2 shows crude TBP and product distillation curve for a typical atmospheric distillation tower. Back end a product TBP curve is above the crude TBP curve and the front end of the product TBP is lower than the crude TBP curve. One should note that the back end of the lighter cut and the front end of the adjacent heavier cut are not equidistant from the crude TBP curve. Similarly, midpoint of a TBP distillation curve for a cut does not lie on the crude TBP distillation curve. Such pattern as a rule appears in practically all industrial CDUs. Unfortunately, vast majority of the published works on simplified crude distillation modelling assume that (i) the back end/front end points of adjacent products are equidistant from the crude distillation curve and (ii) the midpoint of a product distillation curve lies on the crude distillation curve.

1.2 Main contributions

This work developed a high accuracy hybrid model of a crude unit. The model does not rely of the assumptions (i) and (ii). Hence, the model computes correctly product TBP curves that are observed in actual CDUs. In addition, we illustrate how to represent the

crude assay data for this hybrid model and how product and crude TBP curves and property distribution curves can be used to compute bulk properties (e.g. % sulfur) of the product streams. Results computed by the hybrid model are compared with those from a rigorous tray to tray model. Differences between the predictions by the two models are within the error of the analytical instruments used to measure product distillation curves.

The main contributions for this research are:

a) Develop crude assay data modeling in a form required by the CDUs model. This model can also be used for evaluation crude assay data without commercial process simulation software such as Aspen plus, Pro/II, etc.

b) Develop hybrid model of crude distillation unit for TBP prediction. This hybrid model is not based on two widely used assumptions and almost linear except reflux ratio in atmospheric model. The small size and high accuracy of this model can be used in planning, scheduling and RTO.

c) Develop TBP based property prediction method and compare with other swing cut related methods. These property prediction methods show nearly the same prediction accuracy if using right yields which is not based on equidistance assumption. So either of property prediction methods can be integrated with hybrid TBP prediction model which can provide the yields.

1.3 Thesis overview

In section 2, the brief review of the prior work on crude distillation unit related the products properties prediction and application in planning, scheduling and RTO is given.

Section 3 presents a simple way to estimate pseudo-components and properties for each pseudo-components. The crude assay data and crude mix properties can be easily estimated and can be used for further model.

Section 4 describes hybrid CDUs model for TBP prediction in detail including simulation data generation, model developing, and verification.

Section 5 describes computation of other stream properties (e.g. specific gravity and sulphur). Different swing cut methods are evaluated and compared with this TBP based property prediction method.

Section 6 first highlights major accomplishments and result of this research, followed by recommendation for future research.

2. Literature review

In section is to provide a brief review of some prior work relevant to this research. Topics covered in this section include: crude distillation unit and swing cut related property prediction.

2.1 Crude distillation unit

Accurate and robust models capable of predicting CDU product yields and properties took several decades of rigorous distillation tower model developments. Rigorous model uses material and energy balance and liquid vapor equilibrium (LVE) for each tray. So it can provide tray to tray information such as internal flowrate, temperature, etc. Rigorous model is suitable for detail design and real time optimization due to these features. The first commercial flowsheet simulation software capable of solving reliably complex distillation tower models was SSI/100 by Simulation Sciences, which was released in mid 1970s. Boston et al. (1974) published "inside-out" algorithm for rigorous tray to tray simulation of distillation towers, which has become the basis for all present day algorithms for distillation of wide boiling mixtures. In mid-1980's HYSIM introduced the use of property curves, such as % of sulfur, and their mixing via pseudo components to predict product properties other than distillation curves (Svrcek(1989)). This was soon followed by similar development in AspenPlus and Pro/II. Since early 1990s process simulation, design, and real-time optimization applications have relied on these

large scale (10,000 equations or more) nonlinear model capabilities to predict accurately the outcome of processing crude feedstocks under specified set of operating conditions.

In addition to rigorous distillation tower models, commercial simulators usually offer a simplified, fractionation index based models of complex distillation towers (e.g. Aspen Plus 11.1 Unit Operation Models.(2001)). These have been provided to fill the need for easy to configure and easy to tune models of complex distillation towers.

Rigorous distillation models available in simulation software have many equations, are highly nonlinear and are not suitable for use in production planning and scheduling. In order to accomplish reasonable solution times for planning and for scheduling models, crude units have traditionally been represented by various forms of linear and recently simplified nonlinear models of CDU behavior, as described in the next section. RTO on the other hand uses tray to tray rigorous distillation models, which makes them too large for use in planning and scheduling. Bagajewicz et al. (2001) used rigourous model and heat demand-supply diagram to design conventional atmospheric crude units considering pumparound and heat exchange network design.

Production planning and production scheduling models require multiple representations of the same crude unit, either because there are many periods and each period has at least one crude unit, or because the crude unit is represented by several modes of operation.

Two simplifying assumption which as a rule are used in these simplified models are: (i) equidistance between the back end of the lighter cut and the front end of the heavier cut, and (ii) the midpoint of a product TBP curve lies on the crude TBP curve (Watkins (1979)). However, if one examines product distillation curves from actual crude distillation towers (or from rigorous tray to tray simulations), I becomes apparent that both of these assumptions are incorrect and that they introduce significant errors in predictions by the models which rely on them.

In simplified distillation unit models, FUG (Fenske-Underwood-Gilliland) mode is the best-known one. The Fenske equation estimates the minimum number of theoretical stages at total reflux (Fenske (1932)). The Underwood equation estimates minimum reflux for an infinite number of theoretical stages (Underwood (1948)). The Gilliland equation estimates the number of theoretical trays required for a given split with the reflux at a fixed multiplier of the minimum reflux ratio (Gilliland (1940)). Suphanit (1999) developed simplified model for crude distillation include modified FUG model, sider – strippers and side-rectifiers. Gadalla (2006) extended this method using in retrofitting for minimal cost and CO2 emissions. Chen (2008) developed an algorithm to find the light key and heavy key component in simplified CDUs model.

Simplest approach to modelling crude units in a mathematical programming planning model is to represent each cut by its yield and approximate its distillation curve by

a) Adding some "delta differences" ΔTB_i (where *i* can be e.g. 90%, 95%, 99%, 100%) to the crude distillation points at the back end of the product, and

b) Subtracting some delta differences ΔTF_i (where *i* can be e.g. 10%, 5%, 1%, 0%) from the crude distillation points at the front end of the product.

Such approximation is not realistic, since CDU unit can operate under variety of conditions, which leads to different sharpness of separation between adjacent products. In other words, deviations from the crude TBP curves are not constant. In addition, this model assumes that the middle section of the product distillation curve (including 50% midpoint) correspond to the crude distillation curve, which is practically never correct.

Frequently used improvement is to define distinct operating states (modes) that will be employed for the crude unit by Brooks et al.(1999). Each operating state is then characterized by different set of "delta differences" for each product. This approach improves somewhat prediction of the product front end and back end distillation points, but still suffers from the fact that these predefined operating modes cannot represent changes in separation which may be required to optimize product blending for a particular demand pattern. Similarly, middle section of the product TBP curve leads to erroneous computation of other properties.

Alattas and Grossman(2011) derived an approximate nonlinear crude distillation model which uses fractionation indices and proposed that the fractionation indices be tuned for different sets of operating conditions. This fraction index method first introduced by Geddes (1958) and extended applied in crude distillation unit by Gilbert (1966). This is similar to the simplified models used in the process simulators (e.g. AspenPlus) and also is similar to models used by some refining companies in their planning models. They also assumed equidistance between the back end of the lighter cut and the front end of the adjacent heavier cut. Alatas and Grossman (2011) did not publish a comparison of their model with rigorous tray to tray results.

All of the above research efforts have relied on the equidistance assumption and on the assumption that the midpoint of the product TBP curve lies on the crude TP curve. Mahalec and Sanchez (2012) presented a model of an atmospheric pipestill which does not assume equidistance between adjacent (back, front end) pairs and also does not assume that the midpoint of the product TBP curve lies on the crude TBP curve. The model was designed with real time applications in mind. Hence, they assumed that the temperature profile in the towers could be estimated from several available tray temperature measurements. This enabled accurate computation of the internal vapor and liquid flows in the tower in mass units (not mole units) and the internal reflux. Product TBP curves were then computed based on the crude TBP data, product yields,

stripping steam flows, and pumparound duties. The model was demonstrated to predict product TBP pints typically with less than 1% error (for 5% to 95% points on the distillation curve). An example application of the model led to an optimum which was verified as feasible via AspenPlus simulation and it was better that the result computed by optimization of the corresponding rigorous tray to tray model in AspenPlus.

Ochoa-Estopier et al. (2014) presented a review of various efforts to create reduced order crude distillation models. They developed a very accurate neural network based model of a crude distillation unit and compared its results to a rigorous simulation.

2.2 Swing cut method

In refinery planning model, a widely used method is to define a swing cut, i.e. amount of the front end of the heavier cut which is transferred to the back end of the adjacent light cut (or the amount of the back end of the lighter cut which is transferred to the front end of the heavier cut). Purpose of the swing cuts is to approximate product distillation curves. Swing cut is an assumed cut between the two adjacent products, most often with constant properties. The size of the cut is assumed as a fixed ratio (volume or weight based) to the total feed to the distillation tower, or as a TBP interval of specific size. If there are more than one crude present in the feed, then the swing cuts from all crudes are mixed and the resulting "mixed swing cut" is distributed among the adjacent products. Since the assumption is that the properties of each swing cut are constant for

the entire TBP range of the swing cut, this methodology cannot represent accurately the fact that the properties are distributed nonlinearly across TBP intervals.

Once product TBP curve is known, its bulk properties can be computed by the methodology which is used by rigorous simulation models (pseudo components “carry” with them other properties and are blended to compute product bulk properties), as illustrated by Menezes et al.(2013). Menezes et al divided each swing cut into “light part” and “heavy part”. Their approach still leaves open the question of how to determine the size of the cut in relationship to the separation capabilities of the distillation tower.

In order to apply the swing cut methodology one must decide on the amount of the transferred components and on their distillation properties. Zhang et al.(2001) applied swing-cut model by taking into account how fractions of the same distillation points swing between adjacent cuts. Li et al. (2005) employed weighted average of the yield changes by using the weight transfer ratio of each product cut. Guerra et al.(2011)also employed swing cut model. Recognizing the limitations of swing cut methodology, Pinto et al. (2000) and Neiro and Pinto (2004) proposed use of nonlinear models to derive delta models and swing cuts.

3. Crude assay data representation

3.1 Introduction

Crude oil typically consist of large number of compounds, and its chemical compositions is not known, so petroleum refining community has adopted crude characterization in a form of crude assays. This research use widely used pseudo-component method, in which the crude oil is cut into pseudo-components based on boiling ranges. In this thesis, the pseudo-component definition follows rules shown in Tab. 1. This method can easily generate the pseudo-components using for CDUs modeling especially for those without simulation software application.

There are two crude oils for modeling in this research. The light end hydrocarbon and properties show in Tab. 2.The assay data of crude oil 1 and crude oil 2 show in the Tab. 3and Tab.4.

Table 1. The pseudo component definition rules

Boiling-point range	Increment
F	*F*
100 to 800	25
800 to 1200	50
1200 to 1400	100
1400 to 1640	120

Table 2. Light end of crude assay hydrocarbon boiling point

Name	Abbreviation	Normal boiling point (*F*)
Methane	C1	-258.7
Ethane	C2	-127.5
Propane	C3	-43.78
Isobutane	IC4	10.89
N-Butane	NC4	31.1
2-Methyl-Butane	IC5	82.18
N-Pentane	NC5	96.91

Table 3. Crude oil 1 assay data

crude oil 1							
TBP		Light end		API curve		Sulfur curve	
LV%	Temperature (F)	Name	LV%	LV%		LV%	wt%
6.8	130	Methane	0.1	5	90	2	0
10	180	Ethane	0.15	10	68	5	0.01
30	418	Propane	0.9	15	59.7	10	0.013
50	650	Isobutane	0.4	20	52	20	0.05
62	800	N-Butane	1.6	30	42	30	1.15
70	903	2-Methyl-Butane	1.2	40	35	40	1.62
76	1000	N-Pentane	1.7	45	32	45	1.9
90	1255	Water	0	50	28.5	50	2.15
				60	23	60	2.54
				70	18	70	3
				80	13.5	80	3.7
			bulk		31.4		2.3

3.2 Methodology

3.2.1 Crude oil assay data modeling

The procedures for crude oil assay data modeling (take crude oil 1 as an example):

a) Extrapolate the TBP curve for the crude assay data. It is very common lacking the analysis crude assay data of high boiling point range when generating pseudo components based on boiling point ranges (like crude oil 1). So we need to extrapolate the incomplete TBP curve to cover all the boiling point range. Sanchez et al. (2007) reviewed several different probability distribution functions to fit distillation curve of petroleum products. They concluded that the cumulative beta function with 4 parameters can give a good extrapolation. So in this thesis, the beta cumulative density function (Eq. 1) and objective function of Min-Max are used to perform extrapolation of TBP curve of crude oil. The formula for beta cumulative density function is given by Eq. 1. The parameters using in this equation are calculated by Min-Max optimization of the objective function shown in Eq. 2. The procedure for the extrapolation shown in Fig.5. The extrapolation results for crude oil 1 TBP curve are shown in Tab. 5, while the Fig. 6 compares the extrapolated curve with AspenPlus result. We can see that four parameters beta function gives us accurate extrapolation when compared with Aspen plus.

$$f(x,\alpha,\beta,A,B) = \int_A^x \frac{1}{B-A}\frac{\Gamma(\alpha+\beta)}{\Gamma(\alpha)(\Gamma(\beta))}(\frac{x'-A}{B-A})^{\alpha-1}(\frac{B-x'}{B-A})^{\beta-1}dx'. \quad (1)$$

$x \leq B$, where Γ is the standard gamma function. α,β,A,B are the four parameters for the beta function. α and β are positive parameter that control the shape of the distribution. A and B parameters set lower and upper bounds on the distribution and x is the normalize crude oil temperature. f is the beta accumulative density function.

Calculate $LV\%_{pred,i}$ from Eq. 1 using normalized temperature given by Eq. 3 and minimize deviations from the crude assay TBP points by using Eq. 2:

$$Min \max_{i=0}^{n}(LV\%_{pred,i} - LV\%_{assay,i})^2 \quad i = 0...n\ known\ crude\ assay\ data \quad (2)$$

$$TBP_{norm} = \frac{TBP-TBP_{min}}{TBP_{max}-TBPmin} \quad (3)$$

TBP_{norm} *is the normalized crude oil TBP point*

TBP_{min} *and* TBP_{max} *define the range of crude oil TBP points*

b) Use linear interpolation to compute the volumetric percentage of each pseudo component. Once we define the boiling point range for each pseudo component, the volumetric percentage of each pseudo component can be calculated. Fig. 7 compares the results from this procedure with AspenPlus.

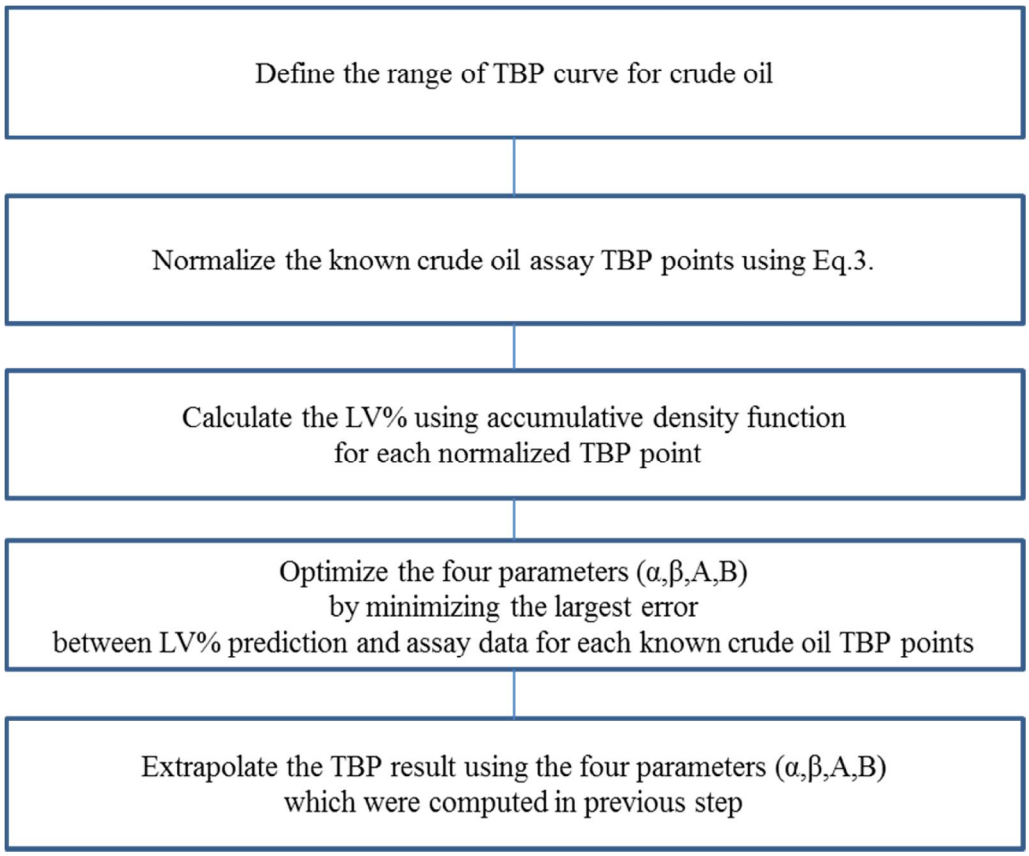

Figure 5. Procedure for beta function extrapolation

c) Use linear interpolation to compute the specific gravity of each pseudo component. The mid-point of the pseudo component TBP range is used as this pseudo component boiling point. The specific gravity can be obtained by linear interpolation of specific gravity curve of crude oil. Fig.8 compares the results with Aspen plus.

d) Use linear interpolation to calculate the sulfur content for each pseudo component. Fig.9 compares the results with Aspen plus.

Table 4. Crude oil 2 assay data

crude oil 2							
TBP		Light end		API		sulfur	
LV%	*Temperature (F)*		*LV%*	*LV%*		*LV%*	*wt%*
6.5	120	Methane	0.2	2	150	2	0
10	200	Ethane	0.5	5	95	5	0.01
20	300	Propane	0.5	10	65	10	0.015
30	400	Isobutane	1	20	45	20	0.056
40	470	N-Butane	1	30	40	30	1.3
50	550	2-Methyl-Butane	0.5	40	38	40	1.7
60	650	N-Pentane	2.5	50	33	45	2
70	750	water	0.1	60	30	50	2.3
80	850			70	25	60	2.7
90	1100			80	20	70	3.2
95	1300			90	15	80	3.8
98	1475			95	10		
100	1670			98	5		
			bulk		34.8		2.5

Table 5. Beta function extrapolation results compared with aspen plus

TBP	aspen plus	beta extrapolate
LV%	*F*	*F*
0	-75.63	1.75
1	-13.01	29.75
5	94.22	104.81
10	180.13	177.27
30	418.26	418.78
50	650.04	650.01
70	903.60	907.00
90	1256.54	1256.42
95	1410.12	1393.42
99	1548.51	1578.60
100	1561.44	1686.45

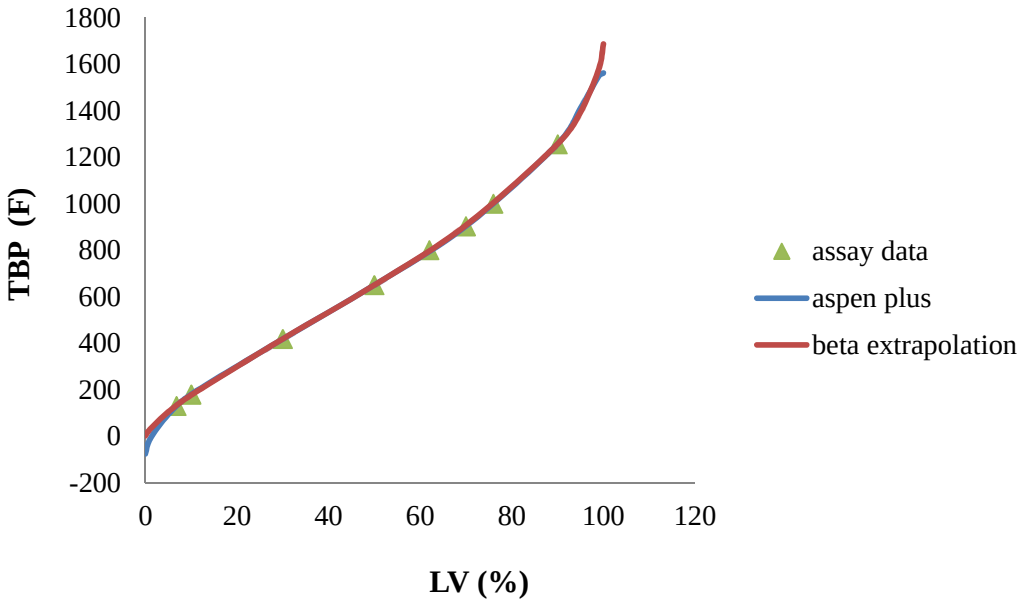

Figure 6. TBP curve extrapolation results for crude oil 1 using beta function

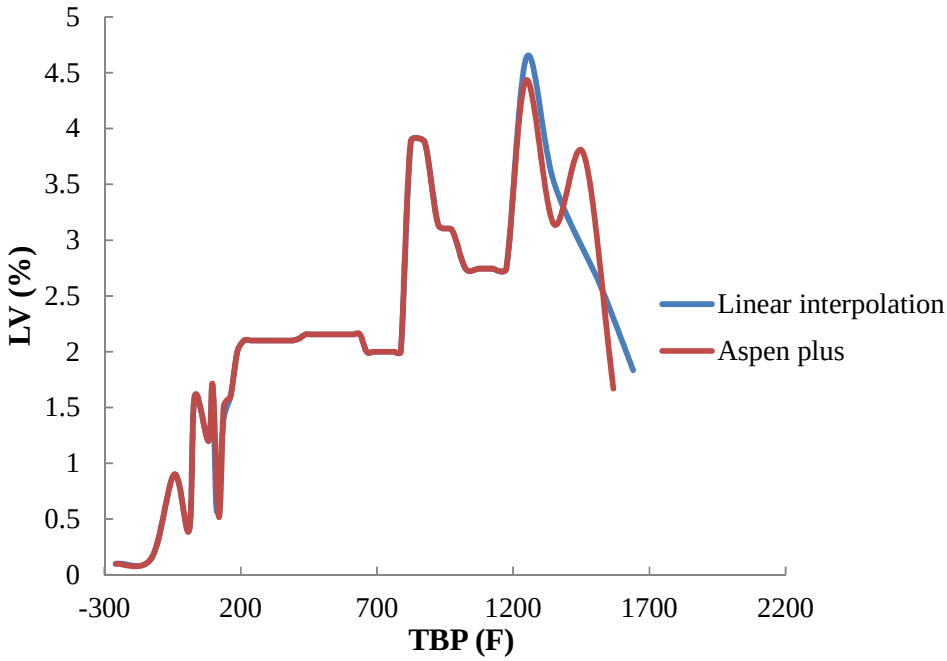

Figure 7. Volumetric percentage for each pseudo component for crude oil 1

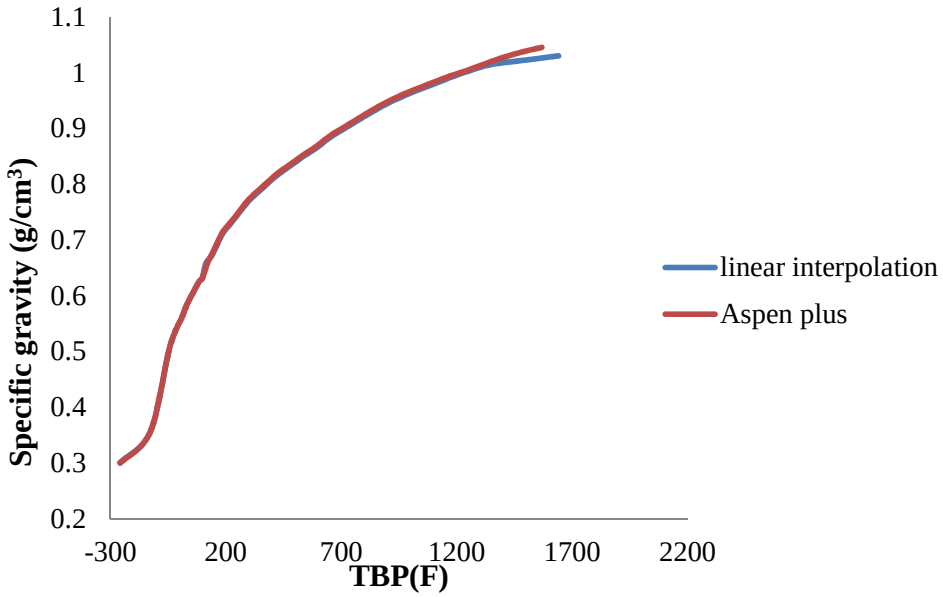

Figure 8. Specific gravity for each pseudo component for crude oil 1

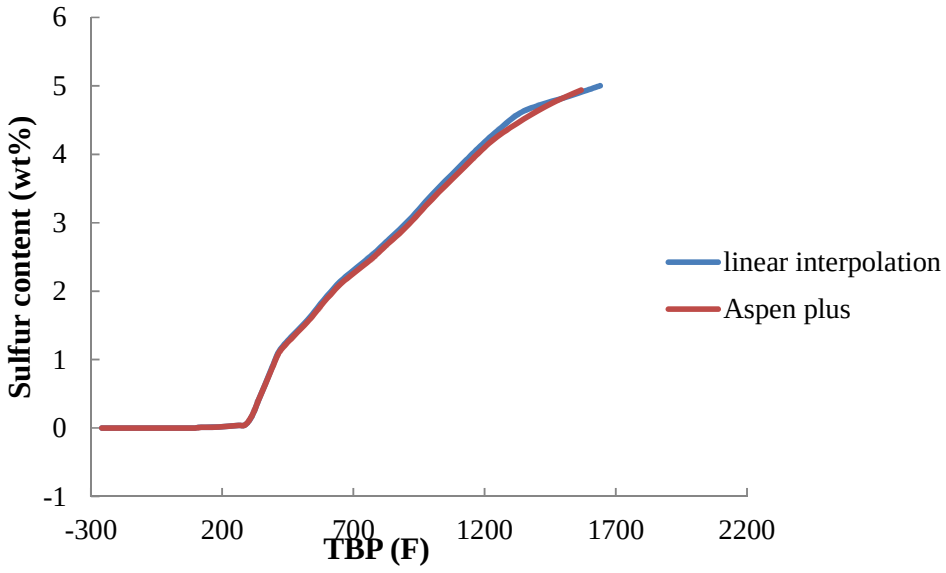

Figure 9. Sulfur content for each pseudo component for crude oil 1

After getting the property distribution curve, the bulk properties can be estimated by accumulating the curve according to the type of properties (volumetric based or mass based). For volumetric based properties (such as specific gravity), Eq. 4 is used. For mass based properties (such as sulfur), Eq. 5 is used.

$$BulkProp_{vol} = \sum_{n}^{i=0} vol_i * Prop_i \quad i = pesudo\,component \tag{4}$$

$$BulkProp_{mass} = \frac{\sum_{n}^{i=0} vol_i * SG_i * Prop_i}{\sum_{n}^{i=0} vol_i * SG_i} \quad i = pesudo\,component \tag{5}$$

3.2.3 crude mix modeling

The procedures for crude oil mix modeling:

Cumulate the volumetric for light end part and each pseudo component to generate TBP curve for crude mix. Eq. 6 is used to calculate the volumetric for each pseudo component. Then TBP curve for the crude mix is calculated by accumulating the volumetric of each pseudo components.

$$vol_i = \sum_{j=0}^{n} vol_{i,j} * fraction_j \tag{6}$$

$i = pesudo\,component;\ j = 1, 2(crude\,oil\,1, crude\,oil\,2),$
$fraction\ means\ the\ fraction\ of\ a\ specific\ crude\ oil\ in\ the\ crude\ mix$

Cumulate volume based properties (such as specific gravity) as Eq. 7.

$$prop_i = \sum_{j=0}^{n} fraction_{vol,j} * prop_{i,j} \tag{7}$$

$i = pesudo\,component;\ j = 1, 2(crude\,oil\,1, crude\,oil\,2)$

Cumulate weight based properties (such as sulfur) as Eq. 8.

$$prop_i = \frac{\sum_n^{j=0} fraction_{vol,j} * SG_{i,j} * prop_{i,j}}{\sum_n^{j=0} ratio_{vol,j} * SG_{i,j}} \quad (8)$$

$i = pesudo\,component;\ j = 1, 2(crude\,oil\,1, crude\,oil\,2)$

Once property curve is obtained, the bulk properties for crude mix can be calculated using Eq. 4 and Eq.5.

3.3 Case study

3.3.1 Crude oil results

There are four different methods used to represent crude assay data. The method includes all scenarios with or without aspen plus data shown in Tab. 6. In the Tab. 6, the middle point means the middle points of each pseudo component range are used as normal boiling point for respective pseudo component. Pricewise linear interpolation is used to calculate the respective pseudo component properties such as TBP, specific gravity and sulfur. For crude oil 1, the TBP, SG, and sulfur prediction comparison shown in Tab 7-9 compared with Aspen plus results. For crude oil 2, the TBP, SG, and sulfur prediction comparison shown in table 10-12 compared with Aspen plus results.

Table 6. Crude oil assay data presentation method

	TBP		SG	Sulfur
	Pseudo	Distribution	Distribution	Distribution
Method 1	n/a	Pricewise Linear interpolation	Pricewise Linear interpolation	Pricewise Linear interpolation
Method 2	Middle point	Aspen plus	Aspen plus	Aspen plus
Method 3	Middle point	Pricewise Linear interpolation	Pricewise Linear interpolation	Pricewise Linear interpolation
Method 4	Aspen plus	Aspen plus	Aspen plus	Aspen plus

Table 7. TBP prediction comparison for crude oi 1

TBP	Aspen plus	method 1	method 2	method 3	method 4
LV%	F	F	F	F	F
1	-13	-58	-58	-58	-58
5	94	88	88	88	88
10	180	180	178	179	178
30	418	418	418	419	418
50	650	650	650	651	650
70	904	903	906	907	905
90	1257	1255	1271	1256	1269
95	1410	1346	1414	1347	1413
99	1549	1419	1573	1420	1561

Table 8. Specific gravity prediction comparison for crude oil 1

SG	Aspen plus	method 1	method 2	method 3	method 4
LV (%)	g/cm^3	g/cm^3	g/cm^3	g/cm^3	g/cm^3
0	0.30	0.57	0.26	0.26	0.26
5	0.63	0.64	0.63	0.63	0.63
10	0.71	0.71	0.71	0.71	0.71
30	0.82	0.82	0.82	0.82	0.82
50	0.88	0.88	0.89	0.88	0.89
70	0.95	0.95	0.95	0.95	0.95

90	1.00	1.01	1.01	1.01	1.01
95	1.03	1.02	1.03	1.02	1.03
100	1.06	1.03	1.05	1.03	1.05
bulk	0.87	0.87	0.86	0.86	0.86

Table 9. Sulfur prediction for crude oil 1

Sulfur	Aspen plus	method 1	method 2	method 3	method 4
LV (%)	*wt%*	*wt%*	*wt%*	*wt%*	*wt%*
0	0.00	0.00	0.00	0.00	0.00
5	0.00	0.01	0.00	0.00	0.00
10	0.01	0.01	0.01	0.01	0.01
30	1.09	1.15	1.10	1.10	1.10
50	2.03	2.15	2.10	2.10	2.10
70	2.83	3.00	2.96	2.96	2.96
90	4.46	4.40	4.31	4.31	4.31
95	5.05	4.75	4.65	4.65	4.65
100	5.59	5.10	4.99	4.99	4.99
bulk	2.26	2.36	2.33	2.33	2.33

Table 10. TBP prediction for crude oil 2

TBP	Aspen plus	method 1	method 2	method 3	method 4
LV (%)	*F*	*F*	*F*	*F*	*F*
1	-38	-77	-77	-77	-77
5	97	90	90	90	90
10	201	200	197	193	197
30	400	400	398	396	398
50	551	550	551	549	551
70	750	750	750	747	750
90	1100	1100	1106	1098	1105
95	1299	1300	1309	1297	1308
99	1525	1573	1563	1552	1553

Table 11. Specific gravity prediction comparison for crude oil 2

SG	Aspen plus	method 1	method 2	method 3	method 4
LV (%)	*g/cm^3*	*g/cm^3*	*g/cm^3*	*g/cm^3*	*g/cm^3*
0	0.30	0.42	0.28	0.28	0.28
5	0.63	0.62	0.63	0.63	0.63
10	0.72	0.72	0.72	0.72	0.72
30	0.82	0.83	0.81	0.82	0.81
50	0.86	0.86	0.86	0.86	0.86
70	0.91	0.90	0.91	0.90	0.91
90	0.98	0.97	0.98	0.97	0.98
95	1.01	0.98	1.01	0.98	1.01
100	1.06	1.00	1.05	1.00	1.05
bulk	0.85	0.84	0.85	0.84	0.85

Table 12. Sulfur prediction for crude oil 2

Sulfur	Aspen plus	method 1	method 2	method 3	method 4
LV (%)	*F*	*F*	*F*	*F*	*F*
0	0.00	0.00	0.00	0.00	0.00
5	0.00	0.01	0.00	0.00	0.00
10	0.02	0.02	0.02	0.02	0.02
30	1.34	1.30	1.29	1.24	1.29
50	2.37	2.30	2.37	2.29	2.37
70	3.30	3.20	3.33	3.21	3.33
90	4.64	4.40	4.57	4.40	4.57
95	5.04	4.70	4.88	4.70	4.88
100	5.38	5.00	5.19	5.00	5.19
bulk	2.48	2.44	2.55	2.43	2.55

3.3.2 Crude mix results

The crude mix prediction results shown in Tab. 13-15 compared with Aspen plus.

Table 13. TBP prediction for mix crude

TBP	Aspen plus	this thesis	this thesis error
LV (%)	*F*	*F*	*%*
1	-32	-71	122.23
5	97	90	-7.56
10	196	193	-1.72
30	403	401	-0.51
50	567	568	0.13
70	772	775	0.42
90	1143	1155	1.02
95	1332	1338	0.50
99	1532	1566	2.22

Table 14. Specific gravity for mix crude

SG	Aspen plus	this thesis	this thesis error
LV (%)	g/cm^3	g/cm^3	*%*
0	0.300	0.405	34.918
5	0.631	0.628	-0.495
10	0.719	0.717	-0.258
30	0.820	0.811	-1.086
50	0.862	0.864	0.175
70	0.913	0.920	0.753
90	0.985	0.989	0.409
95	1.015	1.016	0.113
100	1.055	1.051	-0.348
bulk	0.854	0.851	-0.378

Table 15. Sulfur prediction for mix crude

Sulfur	Aspen plus	mode 3	mode 3 error
LV (%)	*wt%*	*wt%*	*%*
0	0.00	0.00	0.00
5	0.00	0.00	0.00
10	0.02	0.02	22.47
30	1.31	1.25	-4.49
50	2.33	2.31	-0.75
70	3.30	3.27	-0.99
90	4.47	4.52	1.06
95	4.99	4.84	-3.05
100	5.42	5.15	-4.90
bulk	2.44	2.50	2.65

4. Hybrid model for TBP prediction

4.1 Introduction

Sample crude distillation unit (see AspenTech "Getting Started with Petroleum Distillation Modelling" (2006)) used in this research is shown in Fig.1. It consists of a preflash tower, an atmospheric distillation tower, and of a vacuum distillation tower. Rigorous model of this unit is used in this work as a substitute for an actual crude distillation unit. "Plant data" used in this study have been generated from this rigorous model. All volumetric flows are expressed as liquids at the standard conditions; all measurements will be expressed in imperial units, as it is customary in North American refineries.

If each tower in the CDU was carrying out perfect, sharp separation, then the entire feed would be separated into cuts as shown by dashed vertical lines in Fig. 2 and each product would have TBP curve identical to the corresponding section of the crude feed. Note that Fig. 2 represents all products from the CDU. Since separation is not perfect, the actual product distillation curves are represented by S shaped curves as shown in Fig.2.

4.2 Material and energy balances

CDU distillation towers have a significant amount of stripping steam as their feeds. Since water does not mix with hydrocarbons, volumetric or mass balances for

hydrocarbons in each tower will be considered separately from the water balances. Volumetric balances (on a dry basis) for the three distillation towers are:

Preflash tower:

$$F_{feed_{pf}}(dry) = F_{lgh}(dry) + F_{nph}(dry) + F_{feed_{ap}}(dry) \quad (9)$$

Atmospheric pipestill:

$$F_{feed_{ap}}(dry) = F_{hnph}(dry) + F_{kero}(dry) + F_{dsl}(dry) + F_{ago}(dry) + F_{feed_{vp}}(dry) \quad (10)$$

Vacuum pipestill:

$$F_{feed_{vp}}(dry) = F_{lvgo}(dry) + F_{hvgo}(dry) + F_{resid}(dry) \quad (11)$$

Water mass balances are:

Preflash tower:

$$MF_{stm_{pf}} = MF_{water_{pf}} \quad (12)$$

Atmospheric pipestill:

$$MF_{stm_{ap}} + MF_{ss_{kero}} + MF_{ss_{dsl}} + MF_{ss_{AGO}} = MF_{water_{ap}} \quad (13)$$

Vacuum pipestill:

$$MF_{stm_{vp}} = MF_{top-vapor} \quad (14)$$

Energy balances will also be written separately for hydrocarbons and for water.

Preflash tower:

$$F_{feed_{pf}}(dry) * \rho_{feed_{pf}} * h_{feed_{pf}} + Qduty_{pf,fur} = F_{lgt}(dry) * \rho_{lgt} * H_{lgt} + F_{nph}(dry) * \rho_{nph} * h_{nph} + F_{feed_{ap}}(dry) * \rho_{feed_{ap}} * h_{feed_{ap}} + Q_{cond}(dry)_{pf} \quad (15)$$

$$MF_{stm_{pf}} * H_{stm_{pf}} = MF_{water_{pf}} * h_{water_{pf}} + Q_{cond}(water)_{pf} \quad (16)$$

$$Q_{cond}(wet)_{pf} = Q_{cond}(dry)_{pf} + Q_{cond}(water)_{pf} \quad (17)$$

Atmospheric pipestill:

$$F_{feed_{ap}}(dry) * \rho_{feed_{ap}} * h_{feed_{ap}} + Qduty_{ap,fur} = F_{hnph}(dry) * \rho_{hnph} * h_{hnph} + F_{kero}(dry) * \rho_{kero} * h_{kero} + F_{dsl}(dry) * \rho_{dsl} * h_{dsl} + F_{ago}(dry) * \rho_{ago} * h_{ago} + F_{vp-feed}(dry) * \rho_{vp-feed} * h_{vp-feed} + \sum_{k=1}^{2} Qduty_{u,QPA_k} + + Q_{cond}(dry) \quad (18)$$

$$MF_{stm_{ap}} * H_{stm_{ap}} + \sum_{i=1}^{3} (MF_{ss_i} * H_{ss_i}) = MF_{water_{ap}} * h_{water_{ap}} + Q_{cond}(water)_{ap} \quad i = 1, 2, 3(kero, dsl, ago) \quad (19)$$

$$Q_{cond}(wet)_{ap} = Q_{cond}(dry)_{ap} + Q_{cond}(water)_{ap} \quad (20)$$

Vacuum pipestill:

$$F_{feed_{vp}}(dry) * \rho_{feed_{vp}} * h_{feed_{vp}} + Qduty_{vp,fur} = F_{LVGO}(dry) * \rho_{LVGO} * h_{LVGO} + F_{HVGO}(dry) * \rho_{HVGO} * h_{HVGO} + F_{resid}(dry) * \rho_{resid} * h_{resid} + \sum_{k=1}^{2} Qduty_{vp,QPA_k} \quad (21)$$

$$MF_{stm_{vp}} * H_{stm_{vp}} = MF_{top-vapor} * H_{top-vapor} \quad (22)$$

Steam balance for VP tower (Eq.22) assumes that the entire vapor stream from the top of the VP tower is steam.

4.2 Enthalpy calculation

We need to compute unit enthalpies *[energy/mass]* of hydrocarbon streams, energy supplied by the furnace, energy removed by the condenser, and the pumparound duties. We assume that at some base operating conditions we have available bulk thermodynamic properties (stream enthalpy, specific heat capacity, density, and heat of vaporization). Thermodynamic properties at conditions different from the base case are then computed as incremental changes from the base case. We will also assume that the pressure in each distillation tower does not vary significantly from the pressure at the base operating state, as is the case in refinery operations. Computation of energy balances is carried on a dry basis, disregarding steam balances. This does not have an impact on the accuracy of calculation, since the stripping steam flows through the tower without a large change in the steam enthalpy and it is condensed at the top of the tower.

Since the model will be used to predict operation under a variety of conditions, temperatures of the liquid streams leaving e.g. atmospheric distillation tower will vary. If we employ *[energy/mass]* instead of *[energy/mole]*, we will notice that the specific heat capacities of hydrocarbons of similar molecular weights are approximately the same. Therefore, if the composition of a stream varies around some base composition, the

specific heat capacity of the material remains practically constant. For instance, if kerosene 95% point changes by 10 or 20 deg F, there are some changes to its composition but its specific heat capacity remains practically constant. Since rage of changes in operating conditions is relatively small with respect to the base case, we can also assume that the specific heat capacities of individual streams do not vary with temperature when the distillation tower moves from one operating state to another. Therefore, unit enthalpy of a stream can be calculated by Eqs. (15) and (16) for liquid and vapor streams, respectively.

$$h_i = h_i^0 + C_{i,L}(T_i - T_i^0) \tag{23}$$

$$H_i = H_i^0 + C_{i,V}(T_i - T_i^0) \tag{24}$$

Temperature of a stream leaving a side-stripping tower differs from the temperature of the main tower draw-off tray by some difference. This difference changes somewhat from one set of operating conditions to another, but for purposes of energy balance calculations it can be assumed to be constant. Hence, if we can estimate the temperature at the draw-off tray, then we can calculate the temperature of the stream leaving the side-stripping tower. Temperature at the draw-off tray varies with the boiling point of the material on that tray, which is also the same material as the one leaving the main tower and it is closely related to the product stream from the side-stripper. Front end of

the distillation curve of the product stream is heavier than the front end of the material on the draw-off tray, due to additional separation and the steam used in the side-striper. These considerations lead us to a relationship between the draw-off tray temperature, the product cut point temperature, and (stripping steam/product flow) ratio, Eq. (17) for each of the side products i.

$$T_{draw\_off\_tray,i} = a_0 + a_1 * cutt_{ap,i} + a2 * ss_i / y_{ap,i} \quad (25)$$

and the product p stream temperature is then:

$$T_i = T_{draw\_off\_tray,i} + a_3 \quad (26)$$

Heat duty of the condenser for the atmospheric tower can be computed from the heat of vaporization of the distillate and the total liquid leaving the condenser. Maxwell (1932) presented heats of vaporization for hydrocarbons at various pressures, showing that at the pressure of 1 atmosphere the heats of vaporizations of C7 to C10 hydrocarbons are within 5% of each other. Since naphtha composition can vary significantly from one operating state to another, and since the condenser is a very large contributor in the energy balance, heat of vaporization of naphtha needs to be estimated as accurately as possible. Mid-point at the distillate TBP distillation curve T50d is a good surrogate for naphtha composition. We can use linear approximation around the base operating conditions, as shown by Eq. (19), to compute the heat of vaporization of the distillate. Fig. 10 shows

the relation between naphtha TBP 50% point and the latent heat for naphtha. From Fig.10, The straight line is used for regression. The R^2 is only 0.6965, but the error of prediction is about $\pm 5 mbtu/lb$ compared with average value $192 mbtu/lb$, the error is about 2.5%. Fig. 11 shows the comparison of the predicted value of latent heat and the latent heat value from AspenPlus with three different crudes at wide range of operation conditions. Approximated heat of vaporization has at most 2.5% error compared to the rigorous calculation from a comprehensive thermodynamic package.

$$\lambda_d = \lambda_d^0 + a_4 * (TBP_{d,50} - TBP_{d,50}^0) \tag{27}$$

More accurate computation of the latent heat of naphtha can be accomplished by an iterative procedure by estimating naphtha TBP curve from the model, recalculating the heat of vaporization, estimating again naphtha heat of vaporization, etc. until the desired accuracy is achieved. Since the model predictions are already very accurate, such iterations are not necessary and we have verified such conclusion by experiments.

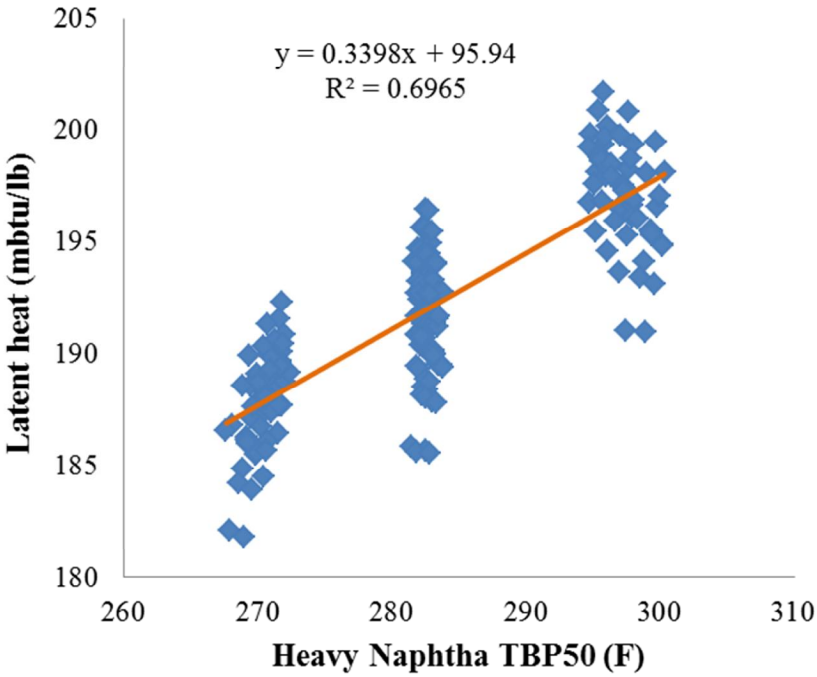

Figure 10. Relationship between naphtha TBP50 and latent heat

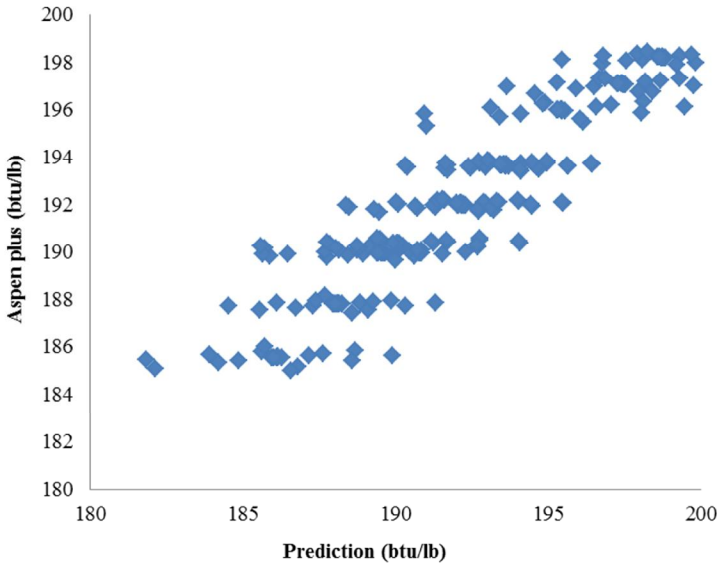

Figure 11. Latent heat approximation VS latent heat computed by AspenPlus

4.3 Methodology

Distillation curves shown in Fig. 12 illustrate that the product distillation curves as a rule do not overlap with the feed distillation curve. This is the case in general, not just for the example model used in this work. Hence, we can not assume that the middle section of the product TBP curve coincides with the feed TBP and then add corrections to the front end and the back end. Such procedure leads to an erroneous product TBP curve which then leads to inaccurate prediction of other properties, since they are computed via their association with the product pseudo component distribution.

Instead of assuming that the middle section of the product TBP curve lies on the feed TBP curve, we need to estimate it from tower operating data, as introduced by Mahalec and Sanchez (2012) (Fig. 12). After that, deviations from the front and the back ends of the line are estimated, as shown in Fig. 12. The procedures for two steps method shown in Fig. 13.

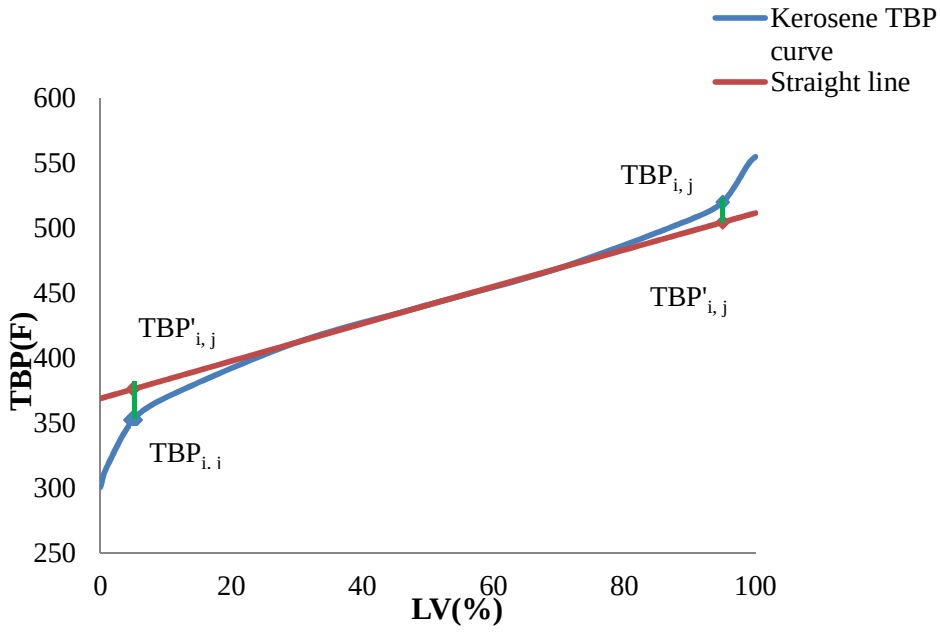

Figure 12. Example of kerosene TBP curve estimation

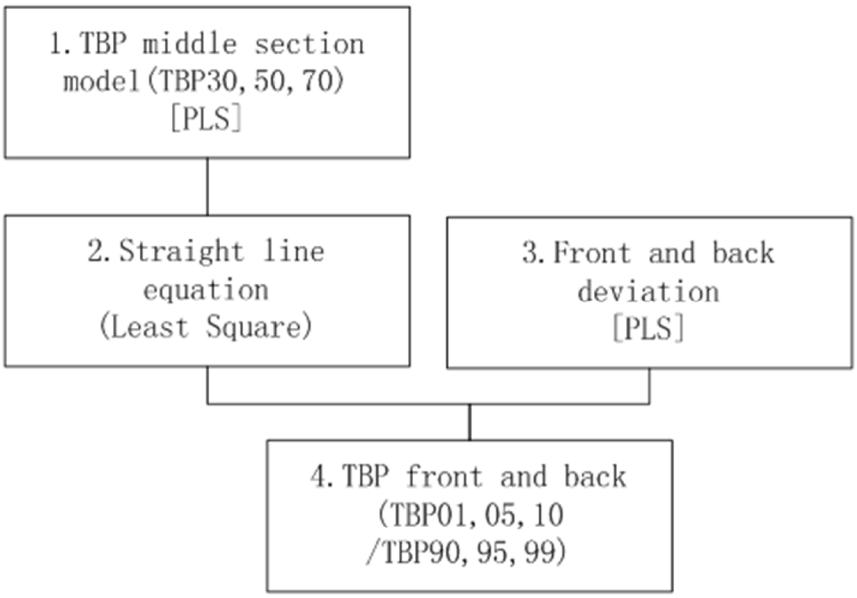

Figure 13. Procedures for two steps method

The middle section of the curve is predicted as by partial least squares (PLS) model using feed TBP curve and the yield of individual products. This section represents how a given distillation tower separates the bulk of the crude among the products, based on the tower structure. It is not directly impacted by changes in other operating conditions, other than through their impact on the yield of individual products. The vertical deviations between the middle section straight line and the front and back sections are predicted by a different PLS model using cut information and operating conditions.

Cumulative cut width of each product ($ccwp_{u,i}$) is defined as:

$$ccwp_{u,i} = \sum_{l=0}^{i}, y_{u,i}/feed_u \tag{28}$$

Then the cut point temperature ($cutt_{u,i}$) of each product can be calculated from the feed TBP curve as shown in Fig. 14.

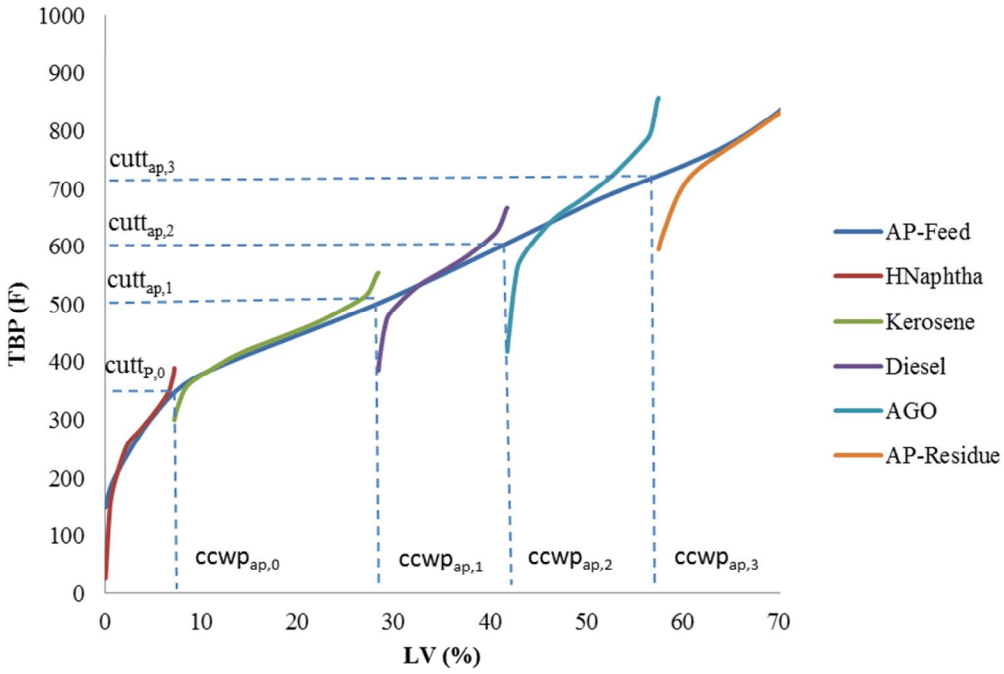

Figure 14. Product cumulative cut width and cut point temperature

Separation in the tower is governed by the number of trays and by the internal reflux. Since in production planning and scheduling we do not know the temperature profile in the tower, the model uses external reflux to determine the separation in the tower. In order to account for the internal vapor flows in the tower, the model uses fraction of the feed that vaporizes at the furnace coil outlet temperature (COT).

4.4 Preflash Tower

Purpose of the preflash tower is to separate the light components from the crude. From planning or scheduling viewpoint, specifying the overhead distillate flowrate is the most

important decision. In order to increase accuracy of the predictions, the model requires the condenser temperature (which can be to be assumed constant for planning and scheduling applications), stripping steam flow and overflash. In addition to product properties, the models calculates furnace COT (see Tab. 16). Alternatively, for use in plant operation, one can specify COT and the model calculates the overflash, as shown in Tab. 17.

Table 16. Preflash tower model: input and output variables

Inputs	Outputs
Mix crude TBP curve	PF Furnace Duty
Mix crude density curve	PF Naphtha TBP curve(30,50,70,90,95,99)
Mix crude flowrate(fixed)	AP Feed TBP curve (1,5,10,30,50,70,90,95,99)
PF Stripper steam flowrate	AP Feed density
PF Condenser temperature(fixed 170 F)	AP Feed flowrate(dry)
PF overflash (fixed 5%)(vol)	AP Feed enthalpy (dry)
PF Distillate flowrate(wet) or PF COT	PF COT or PF distillate flowrate(wet)

Preflash tower model was developed from simulation data for very light crude and for very heavy crude (total of 54 cases). The model was then tested against a crude feed consisting of mixtures of medium crude (total of 27 cases). Range of changes in operating variables is shown in Tab. 18.

Table 17. Alternative specification for the preflash tower model

(C: calculated, S: Specified)

Variables	Spec Option 1	Spec Option 2

PF-feed flowrate	S	S
PF overflash	S	S
PF Steam flowrate	S	S
PF distillate rate flowrate	C	S
PF COT	S	C

Table 18. Range of operating variables and feed compositions

for Preflash data generation and testing

Variables	Perturbation	# of experiments
PF distillation flowrate(wet) [bbl/d]	±10000	3
PF COT [deg F]	±10 F	3
PF Steam flowrate [lb/h]	±2000	3
Dataset for modeling(light and heavy crude)		3*3*3*2=54
Dataset for test(medium crude)		3*3*3*1=27
Total for three different crude mixes (heavy, medium, light)		3*3*3*3=81

Equations to predict product TBP curve of the liquid distillate are as follows:

The straight line through the middle section:

$$TBP_{i,j} = a_{i,j,0} + a_{i,j,1} * TBP_{feed_{pf},10} + a_{i,j,2} * ccwp_{pf,i} + a_{i,j,3} * cutt_{pf,i} \quad (29)$$

$$i = 0(nph)\ j = 30, 50, 70$$

$$TBP_{i,j} = a_{i,j,0} + a_{i,j,1} * TBP_{feed_{pf},30} + a_{i,j,2} * ccwp_{pf,i-1} + a_{i,j,3} * cutt_{pf,i-1} \quad (30)$$

$$i = 1(feed_{ap})\ j = 30, 50, 70$$

The deviations from the straight line are defined as:

$$TBP^{d}_{i,j} = TBP'_{i,j} - TBPi,j \quad i = 1(feed_{ap}) \quad k = 01,05,10 \tag{31}$$

$$TBP^{d}_{i,j} = TBPi,j - TBP'_{i,j} \quad i = 0(nph) \quad k = 90,95,99 \tag{32}$$

The deviations for the front and the back sections are given by:

$$TBP^{d}_{i,j} = a_{i,j,0} + a_{i,j,1} * COT_{pf} + a_{i,j,2} * ccwp_{pf,i} + a_{i,j,3} * cutt_{u,i} + a_{i,j,4} * stm_{pf} \tag{33}$$

$$i = 0(nph) \quad j = 90,95,99$$

$$TBP^{d}_{i,j} = a_{i,j,0} + a_{i,j,1} * COT_{pf} + a_{i,j,2} * ccwp_{i-1} + a_{i,j,3} * cutt_{i-1} + a_{i,j,4} * stm_{pf} + a_{i,j,5} * TBP_{crude,30} \tag{34}$$

$$i = 1(ap - feed)\ j = 01,05,10$$

$$TBP^{d}_{i,j} = a_{i,j,0} + a_{i,j,1} * TBP_{crude,50} + a_{i,j,2} * TBP_{crude,70} + a_{i,j,3} * TBP_{crude,90} \tag{35}$$

$$i = 1(ap - feed) \quad j = 90,95,99$$

TBP curve of the feed to the atmospheric distillation tower is computed by estimating its front end; the remainder is copied from the TBP curve of the preflash tower feed. Results from the model testing are presented in Table 19. Maximum error is for 99 vol% TBP point and this is still less than 1% error.

Table 19. Test results for the preflash model

Product	TBP	R2Y	Q2(cum)	AVERAGE	RMSEE	RMSEP
	Vol(%)			*F*	*F*	*F*
PF-naphtha	30	0.990	0.988	168.5	0.6	0.7
	50	0.990	0.988	237.8	1.0	0.8

	70	0.990	0.988	287.6	0.4	0.4
	90	0.968	0.898	355.6	1.1	1.0
	95	0.968	0.898	380.3	1.5	1.5
	99	0.933	0.592	406.9	3.7	3.5
AP-feed	1	0.996	0.996	198.9	0.6	0.6
	5	0.998	0.998	313.4	0.5	0.5
	10	0.944	0.943	385.3	1.6	1.4
	30	0.999	0.999	538.5	0.5	0.4
	50	1.000	1.000	708.4	0.7	0.8
	70	0.998	0.998	895.8	2.3	1.4
	90	1.000	1.000	1253.8	0.2	0.2
	95	1.000	1.000	1407.3	0.2	0.2
	99	0.965	0.965	1558.6	0.2	0.1

4.5 Atmospheric tower

Input and output variables for the atmospheric distillation tower are shown in Tab. 20. Note that we use ratio [reflux/(reflux + distillate), i.e. R/(R+D)] instead of [reflux/distillate], since it represents more closely the internal reflux in the tower. Energy balance requires that we either specify one of the pumparounds and compute R/(R+D) or specify R/(R+D) and compute the second pumparound. Various options for specifying the model are given in Tab. 21.

Table 20. Input and output variables for atmospheric tower

Input	Output
AP Feed flowrate (dry)	AP HNaphtha TBP curve(50,70,90,95,99)
AP Feed density	AP Kero TBP curve(1,5,10,30,50,70,90,95,99)
AP Feed enthalpy (dry)	AP Diesel TBP curve(1,5,10,30,50,70,90,95,99)
AP HNaphtha flow (dry)	AP AGO TBP curve(1,5,10,30,50,70,90,95,99)

AP Kero flow (dry)	VP Feed TBP curve(1,5,10,30,50,70,90,95,99)
AP Diesel flow (dry)	VP Feed flowrate (dry)
AP QPA1 duty	VP feed density
AP Stripper steam flowrate (SS1,SS2,SS3,steam)	
AP Overflash(fixed 3%)(vol)	
AP QPA2 duty or AP Reflux ratio (R/(R+D))	AP Reflux ratio (R/(R+D)) or AP QPA2 duty
AP AGO flow or AP COT	AP COT or AP AGO flowrate

Data for development of the atmospheric pipestill model have been generated by simulating operation with a light crude feed and with the heavy crude feed for a range of operating variables (192 cases), as shown in Tab.22. The feed was calculated by the rigorous simulation of the preflash tower, since this represented the feed as it would be produced in a real plant. The model was then tested (96 cases) against predictions from rigorous simulations for a mixed crude feed (between the light and the heavy crude). Results of the model testing are shown in Tab. 23. In these tests, all TBP points computed by the hybrid model in these test were less than 1% from the TBP points computed by the rigorous simulation.

Table 21. Alternative specification for atmospheric tower model

(C: calculated, S: Specified)

Variables	Spec Option 1	Spec Option 2	Spec Option 3	Spec Option 4
AP HNaphtha flowrate	S	S	S	S
AP Kero flowrate	S	S	S	S
AP Diesel flowrate	S	S	S	S
AP Overflash	S	S	S	S

AP QPA1 duty	S	S	S	S
AP SS1(Kero) flowrate	S	S	S	S
AP SS2(Diesel) flowrate	S	S	S	S
APSS3(AGO) flowrate	S	S	S	S
AP Steam flowrate	S	S	S	S
AP Reflux ratio (R/(R+D)	S	C	S	C
AP QPA2 duty	C	S	C	S
AP AGO flowrate	C	C	S	S
AP COT	S	S	C	C

Table 22. Perturbations of operating variables and feed compositions

for atmospheric tower data generation

Variables	Perturbation	# of experiments
AP QPA1 duty (*mmbtu/h*)	±40%	3
AP QPA2 duty(*mmbtu/h*)	±40%	3
AP SS1,SS2,SS3 flowrate (*lb/hr*)	±40%	9
AP steam (*lb/h*)&AP COT (*Deg F*)	±40%&±20 *Deg F*	9
Base case, Max Naphtha, Max Kerosene, Max Diesel		4
Dataset for modeling(light and heavy crude)		24*4*2=192
Dateset for test(medium crude)		24*4*1=96
Total for three crude mixes (heavy, medium, light)		24*4*3=288

Product distillation curves are computed from the following equations:

The straight line through the middle section:

$$TBP_{i,j} = a_{i,j,0} + a_{i,j,1} * \rho_{feed_{ap}} + a_{i,j,2} * ccwp_{ap,i} + a_{i,j,3} * cutt_{ap,i} \quad (36)$$

$$i = 0(hnph) \quad j = 50, 70$$

$$TBP_{i,j} = a_{i,j,0} + a_{i,j,1} * \rho_{feed_{ap}} + a_{i,j,2} * ccwp_{ap,i} + a_{i,j,3} * cutt_{ap,i-1} + a_{i,j,4} * cutt_{u,i} \quad (37)$$

$$i = 1, 2, 3(kero, dsl, ago) \quad j = 30, 50, 70$$

$$TBP_{i,j} = a_{i,j,0} + a_{i,j,1} * \rho_{feed_{ap}} + a_{i,j,2} * ccwp_{ap,i-1} + a_{i,j,3} * cutt_{ap,i-1} + a_{i,j,4} * TBP_{feed_{ap},70} \quad i = 4(feed_{vp}) \quad j = 30, 50, 70 \quad (38)$$

where k are points on the distillation curve

The deviations from the straight line are defined as:

$$TBP^{d}_{i,j} = TBP^{'}_{i,j} - TBPi, j \quad (39)$$

$$i = 1, 2, 3, 4(kero, dsl, ago, feed_{vp}) \quad j = 01, 05, 10$$

$$TBP^{d}_{i,j} = TBPi, j - TBP^{'}_{i,j} \quad (40)$$

$$i = 0, 1, 2, 3(hnph, kero, dsl, ago) \quad j = 90, 95, 99$$

The deviations for the front and the back sections are given by:

$$TBP^{d}_{i,j} = a_{i,j,0} + a_{i,j,1} * y_{ap,0} + a_{i,j,2} * y_{ap,1} + a_{i,j,3} * ss_{ap,1}/y_{ap,1} + a_{i,j,4} * \Delta TGap_{i,i+1} + a_{i,j,5} * RefluxRatio \quad (41)$$

$$i = 0(hnph) \quad j = 90, 95, 99 \quad or \quad i = 1(kero) \quad j = 01, 05, 10$$

$$TBP^{d}_{i,j} = a_{i,j,0} + a_{i,j,1} * y_{ap,i} + a_{i,j,2} * y_{ap,i+1} + a_{i,j,3} * ss_{ap,i+1}/y_{ap,i+1} + a_{i,j,4} * \Delta TGap_{i,i+1} + a_{i,j,5} * ccwp_{ap,i} + a_{i,j,6} * \varphi \quad (42)$$

$$i = 1,2,3(kero, dsl, AGO) \quad j = 90,95,99$$

$$TBP_{i,j}^{d} = a_{i,j,0} + a_{i,j,1} * y_{ap,i-1} + a_{i,j,2} * y_{ap,i} + a_{i,j,3} * ss_{ap,i}/y_{ap,i} + a_{i,j,4} * \Delta TGap_{i-1,i} + a_{i,j,5} * ccwp_{ap,i-1} + a_{i,j,6} * \varphi \quad (43)$$

$$i = 2,3,4(dsl, AGO, feed_{vp}) \quad j = 01,05,10$$

$$TBP_{i,j}^{d} = a_{i,j,0} + a_{i,j,1} * ccwp_{ap,3} + a_{i,j,2} * cutt_{ap,3} + a_{i,j,3} * \varphi \quad (44)$$

$$i = 4(feed_{vp}) \quad j = 90,95,99$$

4.6 Vacuum tower

Vacuum pipestill is much simpler that the atmospheric tower. Hence it has a much smaller number of input and output variables, as shown in Tab. 24. There are two possible sets of specifications as presented in Tab. 25. Data for model development have been developed by 276 simulations (light crude, heavy crude, various operating conditions in the atmospheric tower, and the vacuum tower). Tab. 26 summarizes the range of operating conditions used for data generation. The model was tested with 147 additional sets of data for medium mix of crudes in the feed and various operating conditions. Shown in Tab.27 are the test results for the models. Similarly to the atmospheric and preflash tower models, the vacuum tower model predicts TBP points within 1% of the rigorous simulation.

Table 23. Test results for the atmospheric pipestill model

Product	TBP	R2Y	Q2(cum)	AVERAGE	RMSEE	RMSEP
	LV (%)			*F*	*F*	*F*
AP-HNaphtha	50	0.955	0.955	283.3	2.1	0.5
	70	0.982	0.982	312.4	1.7	0.8
	90	0.894	0.865	344.4	0.8	0.9
	95	0.900	0.828	359.5	1.0	1.3
	99	0.968	0.947	380.7	0.8	1.0
AP-Kero	1	0.722	0.708	312.5	2.3	2.2
	5	0.900	0.856	346.8	1.4	1.3
	10	0.785	0.774	364.4	1.2	1.1
	30	0.985	0.985	409.9	0.7	0.5
	50	0.990	0.990	439.5	0.6	0.3
	70	0.995	0.995	468.4	0.7	0.4
	90	0.750	0.732	498.2	0.6	0.6
	95	0.720	0.697	514.6	0.9	0.8
	99	0.600	0.579	536.3	2.8	2.4
AP-Diesel	1	0.955	0.952	403.4	1.4	1.3
	5	0.948	0.946	457.6	1.1	1.1
	10	0.913	0.909	482.0	0.9	0.9
	30	0.997	0.958	532.0	0.5	0.5
	50	0.991	0.970	559.9	0.6	0.6
	70	0.918	0.892	588.6	1.0	1.0
	90	0.799	0.744	624.3	1.1	1.1
	95	0.754	0.690	642.6	1.2	1.1
	99	0.742	0.687	667.4	1.2	1.3
AP-AGO	1	0.972	0.969	454.7	1.3	1.1
	5	0.944	0.939	543.4	1.4	1.0
	10	0.910	0.901	585.5	1.1	0.9
	30	0.964	0.963	647.4	2.1	2.0
	50	0.956	0.955	683.5	2.4	2.2
	70	0.918	0.936	721.9	3.0	2.8
	90	0.882	0.870	773.8	1.7	1.6
	95	0.881	0.869	794.7	2.3	2.3
	99	0.700	0.681	839.9	4.8	5.2
VP-feed	1	0.977	0.976	606.6	1.9	2.0

	5	0.992	0.992	685.0	0.8	1.7
	10	0.985	0.984	733.2	0.8	2.0
	30	0.995	0.994	848.2	1.4	1.7
	50	1.000	1.000	982.8	0.5	7.4
	70	0.999	0.999	1148.0	0.4	6.5
	90	0.959	0.959	1413.5	1.9	0.5
	95	0.940	0.940	1510.7	1.5	1.2
	99	0.999	0.999	1593.7	0.3	2.5

Table 24. Input and output analysis for vacuum tower

Inputs	Outputs
VP Feed flow (dry)	VP Residue flowrate
VP Feed TBP curve	VP LVGO flowrate
VP COT	VP LVGO TBP Curve(1,5,10,30,50,70,90,95,99)
VP Steam flowrate	VP HVGO TBP Curve(1,5,10,30,50,70,90,95,99)
VP Overflash (fixed 0.6%)(vol)	VP Residue TBP Curve (1,5,10,30,50,70,90,95,99)
VP HVGO flowrate or VP QPA2	VP QPA2 or VP HVGO flowrate

Table 25. Alternative specification for vacuum pipestill model

(C: calculated, S: Specified)

Variables	Spec Option 1	Spec Option 2
VP Overflash(fixed)	S	S
VP COT	S	S
VP Steam flowrate	S	S
VP LVGO flowrate	C	C
VP Residue flowrate	C	C
VP QPA1duty	C	C
VP HVGO flowrate	S	C
VP QPA2 duty	C	S

Table 26. Perturbation of operating variables and feed compositions

for vacuum tower data generation

Variables	Perturbation	# of experiments
VP furnace COT (*Deg F*)	±20F	3
VP Steam flowrate (*lb/h*)	±40%	3
VP HVGO flowrate (*bbl/day*)	±40%	3
AP Steam flowrate (*lb/h*) & AP COT(*Deg F*)	±40% & ±20F	4
Dateset for modeling(heavy, medium and light crude)		27*4*3=324
Dataset for test (test crude)		27*4*1=108
Total for heavy, medium, light and test crude mixes		27*4*4=432

TBP curves for the products from the vacuum pipestill are described by Eqs. (38) to (40), which have been obtained by PLS.

$$TBP_{i,j} = a_{i,j,0} + a_{i,j,1} * y_{vp,0} + a_{i,j,2} * TBP_{feed_{vp},01} + a_{i,j,3} * TBP_{feed_{vp},05} + a_{i,j,4} * TBP_{feed_{vp},10} + a_{i,j,5} * TBP_{feed_{vp},30} \quad (45)$$

$$i = 0(lvgo) \quad j = 1, 5, 10, 30, 50, 70, 90, 95, 99$$

$$TBP_{i,j} = a_{i,j,0} + a_{i,j,1} * y_{vp,0} + a_{i,j,2} * y_{vp,1} + a_{i,j,3} * TBP_{feed_{vp},30} + a_{i,j,4} * TBP_{feed_{vp},50} \quad (46)$$

$$i = 1(hvgo) \quad j = 01, 05, 10, 30, 50, 70, 90, 95, 99$$

$$TBP_{i,j} = a_{i,j,0} + a_{i,j,1} * ccwp_{vp,1} + a_{i,j,2} * TBP_{feed_{vp},50} + a_{i,j,3} * TBP_{feed_{vp},70} + a_{i,j,4} * TBP_{feed_{vp},90} + a_{i,j,5} * TBP_{feed_{vp},95} + a_{i,j,6} * TBP_{feed_{vp},99} \quad (47)$$

$$i = 2(resid) \quad j = 01, 05, 10, 30, 50, 70, 90, 95, 99$$

Table 27. Test results for vacuum tower model

Product	TBP	R2Y	Q2(cum)	AVERAGE	RMSEE	RMSEP
	LV (%)			*F*	*F*	*F*
LVGO	1	0.986	0.986	547.1	5.6	5.2

	5	0.995	0.995	609.3	2.8	2.5
	10	0.995	0.995	644.4	2.3	2.0
	30	0.986	0.986	718.3	3.0	2.3
	50	0.984	0.984	765.6	2.7	1.8
	70	0.987	0.987	807.0	2.6	1.8
	90	0.975	0.975	869.9	4.6	2.6
	95	0.969	0.969	903.8	5.5	3.0
	99	0.968	0.968	963.4	6.3	3.8
HVGO	1	0.986	0.986	547.1	5.6	5.2
	5	0.995	0.995	609.3	2.8	2.5
	10	0.995	0.995	644.4	2.3	2.0
	30	0.986	0.986	718.3	3.0	2.3
	50	0.984	0.984	765.6	2.7	1.8
	70	0.987	0.987	807.0	2.6	1.8
	90	0.975	0.975	869.9	4.6	2.6
	95	0.969	0.969	903.8	5.5	3.0
	99	0.968	0.968	963.4	6.3	3.8
Residue	1	0.976	0.976	1011.8	3.8	3.5
	5	0.977	0.976	1096.2	3.6	3.4
	10	0.978	0.978	1140.9	3.5	3.4
	30	0.979	0.979	1246.7	3.2	3.2
	50	0.983	0.983	1341.4	2.4	2.5
	70	0.979	0.978	1436.3	1.9	1.8
	90	0.905	0.904	1546.1	4.4	2.4
	95	0.997	0.997	1602.4	0.9	0.9
	99	0.913	0.913	1650.1	5.4	2.7

4.9 Case studies

Test results presented in this part were for individual distillation towers, e.g. atmospheric pipestill was tested by using the crude feed computed by AspenPlus. In this part we present results of testing the hybrid model of the entire CDU unit, i.e. atmospheric tower

feed is computed by the hybrid model of the preflash tower, and the bottoms product of the hybrid model of the atmospheric tower is the feed to the vacuum tower.

There are totally 4 tests in this section. The detail of each test is as following:

- Test #1: The purpose of this test is to evaluate the TBP properties prediction for different crudes (Heavy, medium and light crude, see Tab. 28). The operating conditions for each crude are getting from AspenPlus under same specifications. (see Tab. 29). Then enter these operating conditions into this hybrid CDU unit to generate results for comparison. The compared results are shown in Tab. 30.

Table 28. Mix ratio for three different crudes

	Mix ratio(Oil1:Oil2)(vol) (API of Oil1:31.4, API of Oil 2:34.8)
Heavy crude	0.8:0.2
Medium crude	0.5:0.5
Light crude	0.2:0.8

Table 29. Specifications for the crude distillation unit

Specification	unit	Specification
PF-naphtha TBP95	*F*	380
AP-hnaphtha TBP95	*F*	360
AP-Kero TBP95	*F*	520
AP-Diesel TBP95	*F*	640
HVGO	*bbl/day*	17000
VP-COT	*F*	860

Table 30. Hybrid models results compared with Aspen plus results for three different crudes

three crude mix		unit	light crude(0.8)			medium crude(0.5)			heavy crude(0.2)		
			Aspen Plus	Hybrid model	Err (%)	Aspen Plus	Hybrid model	Err (%)	Aspen Plus	Hybrid model	Err (%)
PF	PF-COT	*F*	474.8	474.9	0.04	467.1	467.9	0.16	460.9	461.4	0.11
	Naphtha TBP95	*F*	380	377.5	-0.67	380	377	-0.8	380	376.8	-0.84
	AP-Feed TBP05	*F*	332.8	332.1	-0.21	319.3	319.6	0.08	307.2	308.8	0.5
	AP-Feed TBP95	*F*	1434.7	1437.1	0.17	1412.5	1412.4	-0.01	1381.1	1380.3	-0.06
AP	AP-COT	*F*	680	676.9	-0.46	680	673.8	-0.92	680	678.8	-0.18
	AP-HNaphtha TBP95	*F*	360	359.9	-0.04	360	359.8	-0.07	360	361.7	0.46
	AP-Kero TBP95	*F*	520	519.1	-0.17	520	519.4	-0.11	520	519.3	-0.14
	AP-Diesel TBP95	*F*	640	637.8	-0.34	640	637.3	-0.42	640	638.7	-0.2
	AP-Kero TBP05	*F*	349.1	346	-0.89	350.8	348	-0.78	352.1	350.8	-0.38
	AP-Diesel TBP05	*F*	463.7	460.7	-0.63	462.3	458.9	-0.73	461.3	459	-0.5
	AP-AGO TBP05	*F*	541.6	538.5	-0.56	539.7	535.9	-0.71	538.2	537.6	-0.13
VP	LVGO 95	*F*	922.7	920.7	-0.21	886.2	895.2	1.02	874.6	862.3	-1.41
	HVGO 95	*F*	1188.3	1189.8	0.13	1185.8	1188.4	0.22	1181.7	1176.3	-0.46
	HVGO 05	*F*	809.6	809.1	-0.07	792.7	789.1	-0.46	768.9	762.7	-0.81

- Test #2a: The purpose of this test is to evaluate the TBP properties prediction for different product strategies for the light crude. Different specifications based on different production strategies were set up in AspenPlus (see Tab.31). After that

the flows computed by rigorous tray to tray model in AspenPlus were used in the hybrid model and the product TBP curves were computed from the hybrid model. The comparison of the results is shown in Tab. 32. Most of the product TBP are less that 1% away from the rigorous model prediction. An exception if 95% point for Heavy Naphtha, which has an error of 1.3%.

Table 31. Product TBP specifications for test #2, atmospheric tower

	Unit	Max HNaphtha	Max Kerosene	Max Diesel
AP-HNaphtha TBP95	*F*	380	340	360
AP-Kerosene TBP95	*F*	520	540	500
AP-Diesel	*F*	640	640	660

Table 32. Hybrid models results compared with AspenPlus results

for three different production strategies by specified products flowrate

three product strategies	Max HNaphtha			max Kerosene			max Diesel		
	Aspen Plus	Hybrid model	Err (%)	Aspen Plus	Hybrid model	Err (%)	Aspen Plus	Hybrid model	Err (%)
AP-HNaphtha TBP95	380.0	384.9	1.28	340.0	344.4	1.30	360.0	362.9	0.79
AP-Kero TBP95	520.0	519.2	-0.15	540.0	539.8	-0.05	500.0	498.7	-0.27
AP-Diesel TBP95	640.0	639.2	-0.12	640.0	638.2	-0.29	660.0	658.7	-0.20
AP-Kero TBP05	363.4	364.5	0.30	339.4	339.9	0.15	348.8	349.7	0.26
AP-Diesel TBP05	460.6	459.1	-0.33	475.7	473.4	-0.48	450.2	449.0	-0.27
AP-AGO TBP05	538.4	538.0	-0.08	535.1	533.6	-0.26	554.7	551.7	-0.53

- Test #2b: The purpose of this test is to evaluate how accurately the hybrid model predicts the product flows. Product specifications from Tab.31 were used in both hybrid model and rigorous tray to tray model in Aspen Plus. Then the flows from the hybrid model were compared to the flows from AspenPlus model as presented in Tab. 33. Flow of heavy naphtha is up to 3% different from AspenPlus. Flow of kerosene is has 2.4% error for the max diesel operation. All other flows have errors less than 1%
- Test #3: The purpose of this test is to examine AP tower hybrid model performance in an optimization application. The objective function is described by Eq.48. Constraints are presented in Tab.34. We used specification set 4 described in section 4. The optimization problem was solved by using GRG nonlinear solver in excel and AspenPlus model was solve in equation oriented mode by DMO. In order to verify hybrid model for TBP prediction, the hybrid model product flows were entered into AspenPlus. The results are shown in Tab.35. It can be seen that the optimum computed by the hybrid model leads to the operating point which is within the specified constrains The main difference between the two models is that the hybrid model recognizes that maximization of pumparound heat duties is advantageous and increases them to the maximum allowed. AspenPlus model

stopped at a significantly lower pumparound duty which results in the objective function being approx. $ 3.8k per day lower.

$$Z = max(24 * y_{ap,0} + 23.42 * y_{ap,1} + 23.1 * y_{ap,2} + 22.5 * y_{ap,3} - 0.84 * ss_{ap} - 0.60 * ss_{ap,1} - 0.60 * ss_{ap,2} - 0.60 * ss_{ap,3} - 53.95 * Qduty_{ap,fur)} \quad (48)$$

$y_{ap,i}\ means\ yield\ of\ product\ i\ in\ atmospheric\ tower$;
$ss_{ap}\ means\ bottom\ steam\ for\ atmospheric\ tower$;
$ss_{ap,i}\ means\ stripper\ steam\ for\ prodcut\ i\ in\ atmospheric\ tower$;
$Qduty_{ap,fur}\ means\ furnace\ duty\ in\ atmospheric\ tower$
$i = 0, 1, 2, 3(naphtha, kerosene, diesel, AGO)$

Table 33. Hybrid models flowrate results compared with Aspen plus results for three different product strategies by specified product TBP constraints

three product strategies	max HNaphtha			max kerosene			max diesel		
	Aspen Plus	Hybrid model	Err (%)	Aspen Plus	Hybrid model	Err (%)	Aspen Plus	Hybrid model	Err (%)
AP-HNaphtha flowrate(*bbl/day*)	6852	6646	-3.00	4732	4590	-3.00	5727	5584	-2.51
AP-kero flowrate(*bbl/day*)	15577	15903	2.09	20395	20568	0.85	13881	14214	2.40
AP-Diesel flowrate(*bbl/day*)	10838	10790	-0.44	7469	7640	2.30	16284	16213	-0.44
AP-AGO flowrate(*bbl/day*)	12465	12541	0.61	13135	13081	-0.41	9839	9870	0.31
AP-Sum flowrate(*bbl/day*)	45733	45880	0.32	45732	45880	0.33	45731	45880	0.33

Table 34. Constraints for profit optimization problems for AP tower

Constraints	Unit	min	max
mix ratio	*oil1:oil2*	0.2:0.8	0.8:0.2
AP-HNapthpa flowrate	*bbl/day*	6000	20000
AP-Kero flowrate	*bbl/day*	3500	7000
AP-Diesel flowrate	*bbl/day*	6000	20000
AP-AGO flowrate	*bbl/day*	6000	20000
AP-QPA1 duty	*mmbtu/h*	-56	-24
AP-QPA2 duty	*mmbtu/h*	-21	-9
AP-SS1(Kero) flowrate	*lb/h*	1980	4620
AP-SS2(Diesel) flowrate	*lb/h*	660	1540
AP-SS3(AGO) flowrate	*lb/h*	480	1120
AP-Steam(Bottom) flowrate	*lb/h*	7200	16800
AP-reflux ratio	*NA*	0.75	0.88
AP-COT	*F*	670	690
AP-HNaphtha TBP95	*F*	n/a	380
AP-Kero TBP95	*F*	n/a	540
AP-Diesel TBP95	*F*	n/a	660
AP-Kero TBP05	*F*	320	n/a
AP-Diesel TBP05	*F*	450	n/a
AP-AGO TBP05	*F*	530	n/a

- Test #4: The purpose of this test is to generate optimization results using different initial values for AspenPlus optimization. In this test, different initial values were used as initial points in AspenPlus using DMO (SQP algorithm). These initial values were from different production strategies and hybrid model optimization results shown in Tab. 36. Different initial values generated different optimization results shown in Tab. 37. From the table, we also can see that the optimal result is best when the optimal results from hybrid model were set up as initial values. However, the

result is slightly different with hybrid model, that's because some of the quality constraints were slightly violated if importing hybrid model results in AspenPlus and AspenPlus generated results obeyed to all constraints. For example, heavy naphtha TBP95, the hybrid model calculation is 380 F but the value from the rigorous model is 383 F (having exactly the same values of operating variables in hybrid model and in AspenPlus). The optimization process changes the operating conditions to satisfy constraint which is no more than 380 F by reducing the flow rate of heavy naphtha. So the profit was slightly smaller than hybrid model result ($654=1,096,022-1,095,368). Different initial points were also given to hybrid model. Hybrid model always generated the same results using GRG in Excel 2010 shown in Tab. 37.

Table 35. Comparison of hybrid model and AspenPlus optimization results

Variables	Unit	Aspen Plus Base Case	Aspen Plus Optimum	Hybrid Model Optimum	Hybrid Model Opt. evaluated by AspenPlus	Constr. Error (%)
mix ratio	*oil1:oil2*	0.2:0.8	0.2:0.8	0.2:0.8	0.2:0.8	n/a
AP-HNapthpa	*bbl/day*	5705	5881	6710	6710	n/a
AP-Kero	*bbl/day*	16874	16247	18187	18187	n/a
AP-Diesel	*bbl/day*	10654	13139	10328	10328	n/a
AP-AGO	*bbl/day*	12500	12987	13023	13023	n/a
AP-QPA1	*mmbtu/h*	-40	-41	-56	-56	n/a
AP-QPA2	*mmbtu/h*	-15	-15	-21	-21	n/a
AP-SS1(Kero)	*lb/h*	3300	3239	1980	1980	n/a
AP-SS2(Diesel)	*lb/h*	1100	992	660	660	n/a
AP-SS3(AGO)	*lb/h*	800	797	480	480	n/a

AP-Steam(Bottom)	*lb/h*	12000	16800	16338	16338	n/a
AP-reflux ratio	*NA*	0.85	0.86	0.79	0.78	n/a
AP-COT	*F*	680	690	690	691	-0.09
AP-Furnace duty	*mmbtu/h*	198	206	207	207	-0.13
AP-HNaphthaTBP95	*F*	360	364	380	383	-0.77
AP-kero TBP95	*F*	520	517	540	542	-0.33
AP-Diesel TBP95	*F*	640	656	660	664	-0.61
AP-Kero TBP05	*F*	352	354	363	362	0.14
AP-Diesel TBP05	*F*	461	463	476	472	0.81
AP-AGO TBP05	*F*	538	557	548	548	0.03
Profit	*$10^3$$/day*		1,092.19	1,096.04	1,096.02	
Difference from AspenPlus optimum	*$10^3$$/day*			3.85	3.83	

Table 36. Different products initial flowrate for production optimization

	unit	Basic	Max HNaphtha	Max Kerosene	Max Diesel	Hybrid model
Naphtha	*bbl/day*	5705	6851.6	4732.4	5727.1	6710
Kerosene	*bbl/day*	16874.2	15577.4	20395.4	13880.8	18187
Diesel	*bbl/day*	10654	10838.3	7468.9	16283.9	10328
Ago	*bbl/day*	12500	12465.2	13134.9	9839.1	13023

Table 37. Production optimization results using different initial points

Variables	units	Basic initial (Aspen Plus)	max Nph initial (Aspen Plus)	max Kero as initial (Aspen Plus)	Max Dsl initial (Aspen Plus)	Hybrid opt initial (Aspen Plus)	A+ opt results (test 3#)	Hybrid model opt results (test 3#)	Hybrid result (aspen Plus)
Naphtha	*bbl/day*	5977	6863	6060	6584	6584	5881	6710	6710
Kerosene	*bbl/day*	17874	16772	14140	17951	17951	16247	18187	18187
Diesel	*bbl/day*	11175	11515	15744	10382	10382	13139	10328	10328
AGO	*bbl/day*	13231	13103	12309	13336	13340	12987	13023	13023
R/(R+D)		0.86	0.83	0.84	0.79	0.79	0.86	0.79	0.78
QPA1	*mmbtu/h*	-41.43	-41.29	-42.87	-55.99	-55.97	-41.46	-56.00	-56.00

QPA2	*mmbtu/h*	-15.09	-15.09	-15.17	-21.00	-21.00	-15.09	-21.00	-21.00
SS1(Kero)	*lb/h*	3240	3247	3185	1980	1980	3239	1980	1980
SS2(Diesel)	*lb/h*	1092	1093	1085	660	660	992	660	660
SS3(AGO)		797	797	797	480	480	797	480	480
SS4 (Bottom)	*lb/h*	16800	16800	16800	16800	16800	16800	16337	16337
COT	*F*	690.0	690.0	690.0	690.0	690.0	690.0	690.0	690.6
AP-furnace duty	*mmbtu/h*	206	206	206	206	206	206	207	207
Naphtha TBP95	*F*	365	380	366	380	380	364	380	383
Kerosene TBP95	*F*	531	530	505	540	540	517	540	542
Diesel TBP95	*F*	657	658	660	660	660	656	660	664
Kerosene TBP05	*F*	357	366	354	360	360	354	363	362
Diesel TBP05	*F*	474	473	455	470	470	463	476	472
AGO TBP05	*F*	556	556	561	546	546	557	548	548
profit	10^3*$/day*	1092.7	1093.1	1092.1	1092.1	1095.4	1092.2	1096.1	1096.0

5. Product properties prediction based on TBP curve

5.1 Introduction

From the properties curve, we can find that the curve is ‘S’ sharp which is similar to the TBP curve of products. That’s because distillation is a physical process, which is only change the distribution of pseudo-components in products. The properties for each pseudo-component do not change through CDUs. The product TBP provide the information of distribution of each pseudo-component in each product. Once we get the TBP curve for a products, we can use this TBP information to predict the other properties (such as specific gravity or sulfur) using linear interpolation, so linear interpolation strategy based on products TBP curve can be used to predict products properties. For product properties, there are three types of properties, volumetric based like specific gravity, mass based like sulfur content, and index based like pour point index. In this thesis, volumetric based and mass based (specific gravity and sulfur content) will be discussed.

The swing cut method is widely used in refinery planning. Swing cut means some boiling point range for a feed can be merged into light product or adjacent heavy product. Fig.15 shows the definition of the swing cuts for atmospheric tower. From the figure, we can find that swing cut of naphtha and kerosene is located between naphtha and kerosene. When making production plan, the swing cut can be merged into naphtha or kerosene

which depends the objective function. For example, the swing cut between naphtha and kerosene is considered as naphtha if the price of naphtha is higher than kerosene. In this way, more profit will be earned. When talking about swing cuts, two important things needed to be considered. One is the size of swing cut; the other is property of swing cut. Three different swing cut methods are used for comparison with TBP based property prediction method. They are fix swing cut method, WTR/VTR swing cut method, and Light and Heavy swing cut method. Here a brief explanation of these three swing cut methods is given.

a) Fixed swing cut method. This method is widely used in planning models. The swing cut size and properties are fixed for this method. According to Zhang(2001), the typical size of the swing cut is 5%, 7% and 9% respectively for swing cut between naphtha and kerosene, kerosene and diesel, and diesel and AGO. The properties of a swing cut can be estimated using the middle point of this swing cut in the piecewise linear interpolation of the properties curve of atmospheric tower feed (shown as asterisk points in Fig. 15).

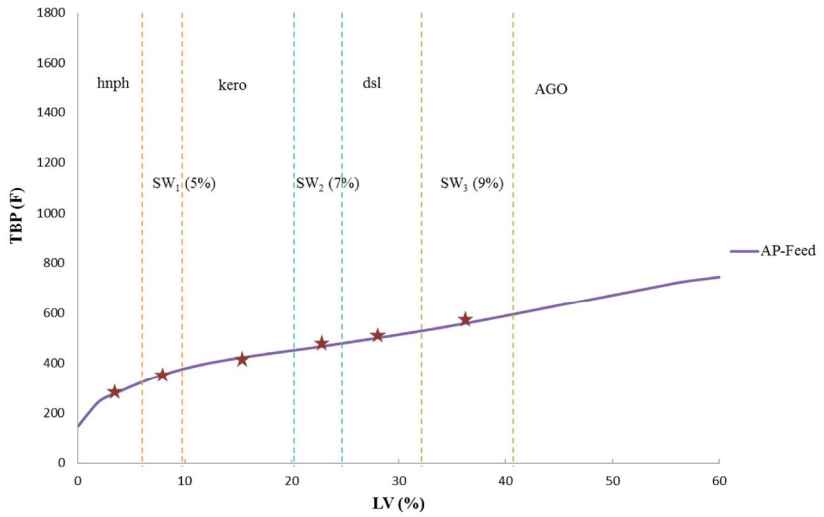

Figure 15. Fix swing cut method

b) Volume transfer ratio/weight transfer ratio (VTR/WTR) method. This method is used for calculated the swing cut size, and the properties of product using empirical correlation of properties curve of atmospheric tower feed. As long as known discrete production strategies (max naphtha, max kerosene, max diesel) are used in CDU operation, we can calculate the swing cut for each product. Take heavy naphtha as an example, the range of naphtha is 8.7% (for max naphtha mode of operation) to 5.9% (for max kerosene mode of operation), then the range of swing cut between naphtha and kerosene is from (5.9% to 8.7%). So the swing cut size is 2.8% (8.7%-5.9%). The hydrocarbons in this range can be become a part of either naphtha or kerosene. Then after getting the yield of each product, the property of each product can be estimated using middle point of each product.

Take heavy naphtha as an example, the middle point of 4% is used for properties calculation if the yield of heavy naphtha is 8% shown as asterisk point in Fig.16.

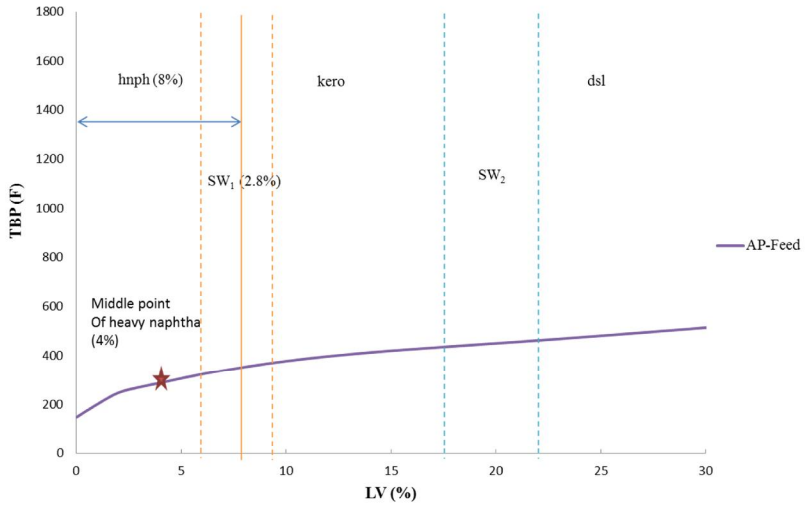

Figure 16. VTR/WTR method

c) Light and heavy swing cut method. The swing cut size is used as in the fixed swing cut method, and the properties calculation of the swing cut is divided into two parts, called light and heavy part. For each of these two parts, the properties can be estimated using middle point of that part piecewise linear interpolation of the properties curve of atmospheric tower feed. In Fig.17, the swing cut between heavy naphtha and kerosene is 5% (from 6% to 11%). The yield of heavy naphtha is 9%, which includes 6% (fixed part) plus 3% (from swing cut). Then the swing cut was divided into two part, the front 3% and the back 2%. In order to calculate

the properties of heavy naphtha, 3% (middle of 6% fix naphtha yield) and 7.5% [6% (fix part) plus middle point of 3% within swing cut] were used.

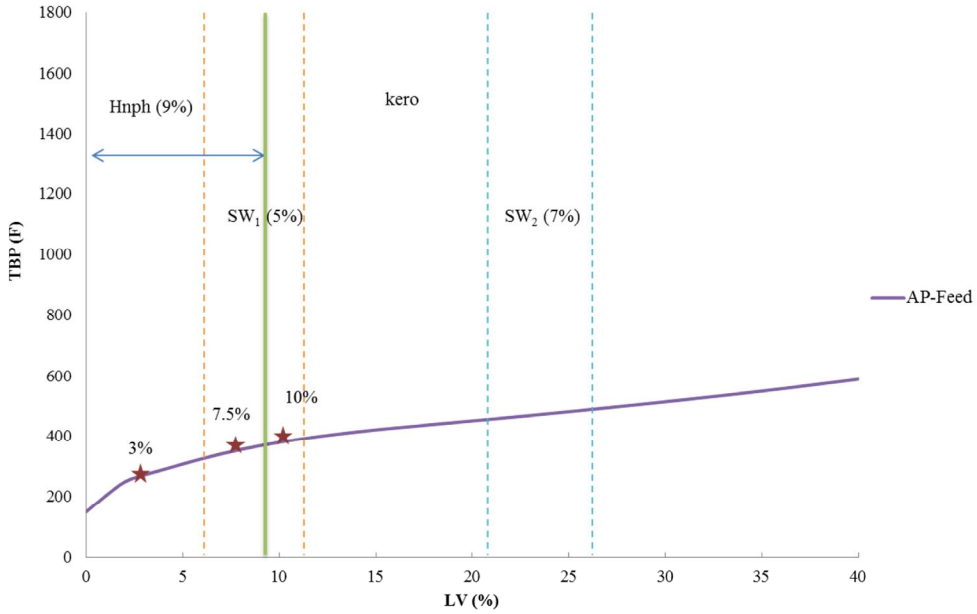

Figure 17. Improved swing cut method

5.2 Methodology

There are four steps for production properties:

a) Calculate the product volumetric based properties curve (specific gravity and sulfur) by linear interpolation each TBP point of this product on mix crude specific gravity curve as Eq. 49. Piecewise linear interpolation is used to calculate specific gravity for each product. Because only discrete point on the properties curve of mix crude(TBP01,05,10,30,50,70,90,95,99), so we simply assume the

section between each discrete point is linear and use one straight line to represent it.

$$SG_{i,j} = Piecewise\,linear\,interpolation(TBP_{i,j}, SG_{mixcrude}) \quad (49)$$

$i = product, j = 1\%, 5\%, 10\%, 30\%, 50\%, 70\%, 90\%, 95\%, 99\%$
$SG_{i,j}\ means\ specific\ gravity\ for\ product\ i\ at\ TBP\ j\ point$
$TBP_{i,j}\ means\ product\ i\ at\ TBP\ j\ point$
$SG_{mixcrude}\ means\ specific\ gravity\ curve\ for\ mixcrude$

b) Calculate the product mass based properties curve (sulfur) by linear interpolation each TBP point of this product on mix crude sulfur gravity curve as Eq.50. Piecewise linear interpolation is used to calculate properties. Because only discrete point on the properties curve of mix crude (TBP 01, 05, 10, 30, 50, 70, 90, 95, 99), so we simply assume the section between each discrete point is linear and use one straight line to represent it.

$$Sulfur_{i,j} = Piecewise\,linear\,interpolate(TBP_{i,j}, Sulfur_{mixcrude}) \quad (50)$$

$i = products(naphtha, kerosene, diesel, AGO)$
$j = 1\%, 5\%, 10\%, 30\%, 50\%, 70\%, 90\%, 95\%, 99\% on\ TBP\ curve$
$SG_{i,j}\ means\ sulfur\ content\ for\ product\ i\ at\ TBP\ j\ point$
$TBP_{i,j}\ means\ product\ i\ at\ TBP\ j\ point$
$SG_{mixcrude}\ means\ sulfur\ content\ curve\ for\ mixcrude$

c) Calculate the bulk volumetric property of the product by accumulation that properties curve by volume as Eq. 51. For property prediction, only fractions from TBP 1% to 99% are used, so denominator is 98($98 = 99 - 1$).

$$SG_i = \frac{\sum_j ((SG_{i,j+1} + SG_{i,j}) * (LV_{j+1} - LV_j))/2}{98} \quad (51)$$

$i = products(naphtha, kerosene, diesel, AGO)$
$j = 1\%, 5\%, 10\%, 30\%, 50\%, 70\%, 90\%, 95\%, 99\%$
$SG_{i,j}\ mean\ specific\ gravity\ for\ prodcut\ i\ on\ TBP\ j\ point$

d) Calculate the bulk mass property of the product by accumulation that properties curve by weight as Eq. 52. For property prediction, only fractions from TBP 1% to 99% are used, so denominator is 98 ($98 = 99 - 1$).

$$Sulfur_i = \sum_i \frac{(SG_{i,j+1} + SG_{i,j}) * (LV_{j+1} - LV_j)/2 * (sulfur_{i+1,j} - (sulfur_{i,j})/2}{SG_i * 98} \quad (52)$$

$i = products(naphtha, kerosene, diesel, AGO)$
$j = 1\%, 5\%, 10\%, 30\%, 50\%, 70\%, 90\%, 95\%, 99\%$
$Sulfur_{i,j}\ mean\ specific\ gravity\ for\ prodcut\ i\ on\ TBP\ j\ point$

5.3 Case study

Crude unit model describe in AspenPlus (2006) manual on petroleum process modelling is used in these case studies. TBP based property prediction method which uses the hybrid model results is compared with fixed swing cut method, weight transfer ratio method, light /heavy swing cut, and with the rigours results generated by AspenPlus.

Three sets of test have been carried out for four different modes of operation (standard operation, maximum naphtha, maximum kerosene, and maximum diesel). The results are presented in English system of units, since they are prevalent in refinery operations in North America.

- **Test #1: verification of hybrid model prediction accuracy for TBP curves.**

TBP 5% point and TBP 95% points of each products were specified in AspenPlus tray to tray model to obtain the volumetric flowrate of each product. Details of the specifications are shown in Tab.38, which is different with only the TBP 99% specification for each products in AspenPlus by Li et al. (2005). The initial boiling points (IBPs), final boiling points (FBPs), and the flowrates were calculated by AspenPlus (Tab.39 and Tab.40 respectively). These product flowrates, stripping steam flows, pumparound duties and reflux/(reflux + distillate)] were inputs to the hybrid model which computed its own predictions of the product TBP curves. Tab.41 compares the results from the hybrid

model with the rigorous AspenPlus model. TBP points computed by the hybrid model are less than 0.5% different from the results of AspenPlus rigorous CDU model. The only exception is the LV% point for naphtha.

Table 38. Specifications for four different modes of operation

		Unit	HNaphtha	Kerosene	Diesel	AGO
Standard	TBP05	*F*	n/a	350	460	540
	TBP95	*F*	360	520	640	n/a
Max HNaphtha	TBP05	*F*	n/a	360	460	540
	TBP95	*F*	380	520	640	n/a
Max Kerosene	TBP05	*F*	n/a	330	470	540
	TBP95	*F*	340	540	640	n/a
Max Diesel	TBP05	*F*	n/a	350	460	560
	TBP95	*F*	360	520	660	n/a

Table 39. IBPs and FBPs for each product

		unit	HNaphtha	Kerosene	Diesel	AGO
Standard	TBP01	*F*	43.1	309.6	406.0	448.3
	TBP99	*F*	380.3	550.0	664.6	n/a
Max HNaphtha	TBP01	*F*	60.6	320.7	406.3	448.3
	TBP99	*F*	400.9	550.0	664.6	n/a
Max Kerosene	TBP01	*F*	28.4	280.6	411.5	449.6
	TBP99	*F*	361.1	564.4	662.9	n/a
Max Diesel	TBP01	*F*	43.2	309.7	403.0	467.2
	TBP99	*F*	43.1	309.6	406.0	448.3

Table 40. Products flowrate for four production modes

	unit	HNaphtha	Kerosene	Diesel	AGO
Standard	*bbl/day*	5618	16934	10707	12458
Max HNaphtha	*bbl/day*	6704	15729	10849	12436

Max Kerosene	*bbl/day*	4318	20784	7605	13010
Max Diesel	*bbl/day*	5620	16813	13109	10175
Max	*bbl/day*	6704	20784	13109	13010
Mix	*bbl/day*	4318	15729	7605	10175
Standard	*LV%*	7.1	21.3	13.5	15.7
Max HNaphtha	*LV%*	8.4	19.8	13.6	15.6
Max Kerosene	*LV%*	5.4	26.1	9.6	16.3
Max Diesel	*LV%*	7.1	21.1	16.5	12.8
Max	*LV%*	8.4	26.1	16.5	16.3
Mix	*LV%*	5.4	19.8	9.6	12.8

Table 41. TBP prediction results by hybrid model compared with Aspen plus

		unit	HNaphtha	Kerosene	Diesel	AGO	Residue
Aspen Plus	TBP01	*F*	43.1	309.6	406.0	448.3	620.4
	TBP05	*F*	122.8	350.0	460.0	540.0	692.8
	TBP95	*F*	360.0	520.0	640.0	798.8	1509.3
	TBP99	*F*	380.3	550.0	664.6	850.8	1587.1
Hybrid Model	TBP01	*F*	44.8	311.0	403.3	445.9	617.1
	TBP05	*F*	123.5	349.3	457.9	538.7	690.3
	TBP95	*F*	361.1	519.3	639.2	800.5	1513.7
	TBP99	*F*	382.5	549.0	663.7	850.9	1605.9
Error	TBP01	*%*	-3.71	-0.44	0.67	0.54	0.55
	TBP05	*%*	-0.49	0.19	0.47	0.24	0.37
	TBP95	*%*	-0.31	0.14	0.12	-0.21	-0.29
	TBP99	*%*	-0.58	0.19	0.13	-0.02	-1.17

- **Test #2: Evaluation of error introduced by equidistance assumption**

Previously published simplified CDU models rely on the assumption that the crude TBP is in the middle of the distance between FBP and IBP of the TBP curves of the adjacent products. Four different modes of operation (standard, max naphtha, max kerosene, and

max diesel) are used to test this assumption. Results from the rigorous model (Tab.42) were used to calculate the midpoint of adjacent products. For instance, under standard operation kerosene 99% TBP point is 550.0, while diesel 1% TBP is 406.0. The middle point between them is 478.0 as shown in Tab. 42. Equidistance assumption means that the cutpoint between kerosene and diesel corresponds to the 478 F point on the crude TBP curve, which is 24.6 LV% as shown in Tab. 43. Rigorous CDU simulation shows that the cutpoint between kerosene and diesel is actually at 28.3 LV%, i.e. the error is 3.7% of the crude volume which correspond to 17% error in the kerosene yield. Complete comparison for all four modes of operation is presented in Tab.43. It can be seen that errors in product yields are significant for kerosene, diesel, and AGO shown in Fig. 18.

Table 42. Middle point of adjacent products TBP curve

		unit	Cut point (hnph-kero)	Cut point (kero-dsl)	Cut point (dsl-AGO)
Standard	middle point	*F*	344.9	478.0	556.4
	overlap	*F*	70.6	144.0	216.2
Max HNaphtha	middle point	*F*	360.8	478.2	556.5
	overlap	*F*	80.2	143.7	216.4
Max Kerosene	middle point	*F*	320.8	488.0	556.2
	overlap	*F*	80.5	152.9	213.3
Max Diesel	middle point	*F*	345.0	476.6	576.1
	overlap	*F*	70.5	147.3	217.9

Table 43. Cumulative product cutpoints based on equidistance assumption vs. actual

		unit	hnph-kero	kero-dsl	dsl-AGO
Standard	Equidistant midpoint	*LV%*	7.6	24.6	35.3
	Actual (AspenPlus)	*LV%*	7.1	28.3	41.8
	Difference	*%*	0.6	-3.7	-6.5
Max HNaphtha	Equidistant midpoint	*LV%*	8.7	24.7	35.3
	Actual (AspenPlus)	*LV%*	8.4	28.2	41.8
	Difference	*%*	0.3	-3.5	-6.5
Max Kerosene	Equidistant midpoint	*LV%*	5.9	26.1	35.3
	Actual (AspenPlus)	*LV%*	5.4	31.5	41.1
	Difference	*%*	0.5	-5.4	-5.8
Max Diesel	Equidistant midpoint	*LV%*	7.6	24.4	37.8
	Actual (AspenPlus)	*LV%*	7.1	28.2	44.7
	Difference	*%*	0.6	-3.7	-6.9

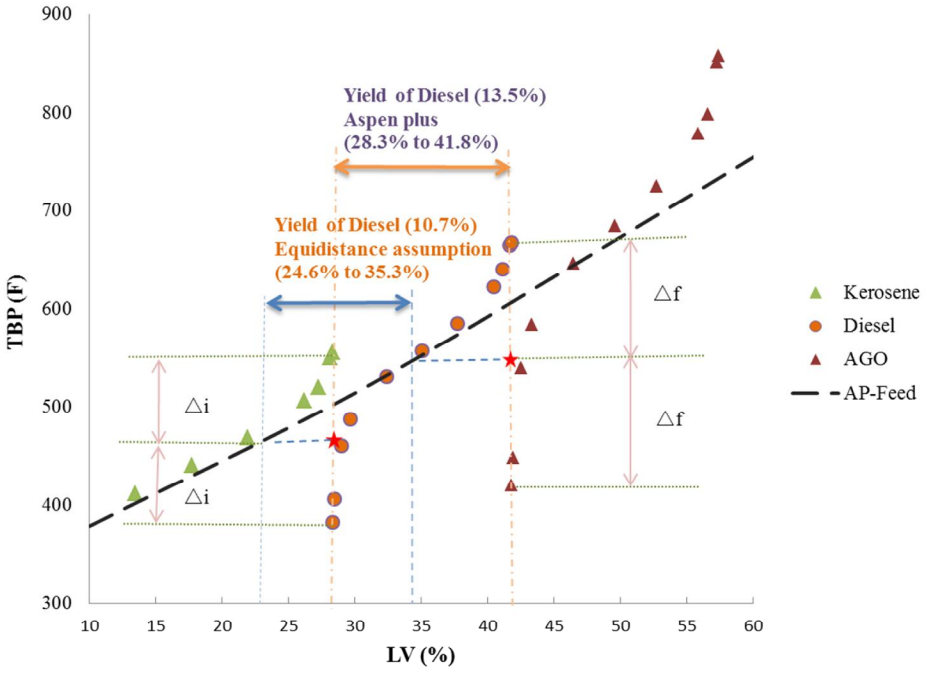

Figure 18. Yield result compared equidistance with AspenPlus

- **Test #3: Evaluation of methods to compute product bulk properties**

There are four test cases in this test as shown in Tab.44. The typical size of the swing cut as introduced by Zhang (2001) is used in this thesis. Swing cut between naphtha and kerosene is 5%, between kerosene and diesel is 7%, and between diesel and AGO is 9%. In this case study, volumetric transfer ratio (VTR) is used because the volumetric flowrates are used. In case 1("fixed cut"), the size and the properties of swing cut are fixed. In case 2 ("VTR"), the size of swing cut is calculated by VTR. The properties are determined by high order polynomial correlations. In case 3 ("L/H cut"), VTR is used due to volumetric flowrate. In case 3, the size of the swing cut is fixed, but the properties of this swing cut are separated into light and heavy part. The properties of light and heavy part are calculated as a linear relationship between the properties at their adjacent hypothetical interfaces.

For "fixed cut" and "L/H cut" methods properties are computed by blending the swing cut properties with the bulk of the corresponding product. In case 4 (this work, "TBP"), the size of the swing cut does not need to be specified; properties are calculated as described above.

Tab. 45 shows yield, specific gravity, and % sulphur for the middle section and the cuts corresponding to each product. These data were used to compute product properties

shown in Tab.46 and Tab.47 (specific gravity and % sulphur, respectively). Also shown in these tables are the results from the rigorous model in AspenPlus and from the TBP method described in this thesis. For data used in this work, for monotonically increasing property (e.g. specific gravity), error relative to AspenPlus is approximately the same for all for cases (four methods of computing cuts and product properties), see Tab. 46. Properties which do not increase monotonically with (LV%, TBP) points (e.g. sulphur) are predicted much more accurately by using TBP method combined with the accurate TBP predictions from the hybrid model, as illustrated by Tab. 47. Distribution specific gravity is shown in Fig.19, while sulphur distribution is shown in Fig. 20.

Table 44. The methodology used in four cases

Case	Swing cut size	Properties	Source
1.fixed cut	fixed	fixed	Zhang(2001)
2.VTR	VTR\WTR	empirical correlation	Li(2005), Guerra(2011)
3.L/H cut	fixed	Mixing of light\heavy parts of each cut	Menezes(2013)
4.TBP cuts	NA	TBP based	This thsis

Table 45. Product properties computed by different swing cut methods

	fixed cut				VTR			L/H cut			
	Size	yield	SG	sulfur	yield	SG	Sulfur	size	yield	SG	Sulfur
	LV%	*LV%*	*g/cm3*	*wt%*	*LV%*	*g/cm3*	*wt%*	*LV%*	*LV%*	*g/cm3*	*wt%*
naphtha	3.0	7.6	0.74	0.03	7.6	0.77	0.05	3.0	7.6	0.74	0.03
sw1-l	4.6		0.79	0.23				4.6		0.79	0.21
sw1-h	0.4		0.79	0.23				0.4		0.80	0.64
kerosene	14.0	17.0	0.82	1.36	17.0	0.82	1.40	14.0	17.0	0.82	1.36
sw2-l	2.6		0.84	1.78				2.6		0.84	1.68

sw2-h	4.4		0.84	1.78				4.4		0.84	1.84
diesel	5.0	10.7	0.85	2.07	10.7	0.85	1.99	5.0	10.7	0.85	2.07
sw3-l	1.3		0.86	2.38				1.3		0.86	2.23
sw3-h	7.7		0.86	2.38				7.7		0.87	2.40
AGO	14.4	22.1	0.89	2.78	22.1	0.88	2.64	14.4	22.1	0.89	2.78

Table 46. Specific gravity predictions vs. AspenPlus

Specific gravity	unit	hnph	kero	dsl	AGO
AspenPlus	*g/cm3*	0.763	0.827	0.858	0.889
fixed cut	*g/cm3*	0.769	0.824	0.848	0.879
VTR	*g/cm3*	0.766	0.824	0.848	0.879
L/H cut	*g/cm3*	0.769	0.824	0.848	0.879
TBP cuts	*g/cm3*	0.754	0.823	0.858	0.894
fixed cut error	*%*	0.820	-0.369	-1.153	-1.154
VTR error	*%*	0.443	-0.394	-1.170	-1.112
L/H error	*%*	0.750	-0.412	-1.147	-1.105
TBP cut error	*%*	-1.154	-0.497	-0.033	0.515

Table 47. Sulfur prediction vs. AspenPlus

sulfur content	unit	hnph	kero	dsl	AGO
AspenPlus	*wt%*	0.17	1.49	2.23	2.83
fixed cut	*wt%*	0.16	1.40	1.99	2.64
VTR	*wt%*	0.05	1.40	1.99	2.64
L/H cut	*wt%*	0.14	1.39	2.00	2.65
TBP cuts	*wt%*	0.20	1.46	2.21	2.83
fixed cut error	*%*	-9.67	-5.80	-10.65	-6.56
VTR error	*%*	-70.58	-5.74	-10.79	-6.63
L/H error	*%*	-19.75	-6.31	-10.38	-6.29
TBP cut error	*%*	18.82	-1.54	-0.92	0.01

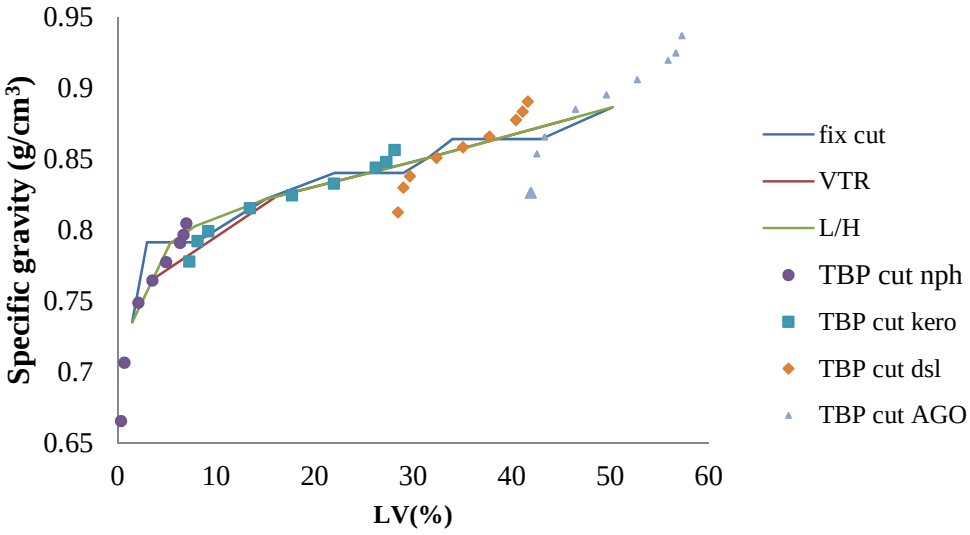

Figure 19. Specific gravity of products using yield based on equidistance assumption

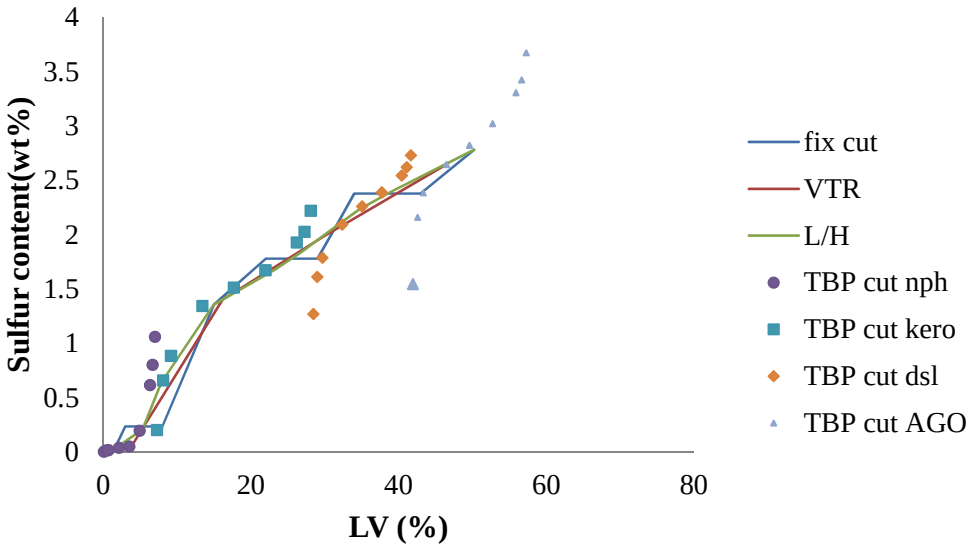

Figure 20. Sulfur content of products using yield based on equidistance assumption

- **Test #4: What is the major source of error for swing cut methods?**

Since there is a fairly large error in computing product yields via swing cut methods, this test is to evaluate its impact on the accuracy of the product properties predictions. There are 6 TBP constraints, we just have 4 manipulate variables. So I try to find the solutions which give TBP as close as possible. The TBP constraint results shown in Tab. 48 and the flowrate compared with AspenPlus shown in Tab. 49 . Instead of using product cumulative cuts (cumulative yields) from the swing cut methods, we substituted the yields from the hybrid model and from them calculated the corresponding (swing) cuts, as shown in Tab.50. In order to compared with previous results, I fix the stripper steam the same as AspenPlus. Then TBP constraints were specified and the yields were manipulated variables. There is not enough freedom to generate the yields exactly the same as AspenPlus.

For instance, for VTR method, the yield of kerosene changed from 17.0% to 21.5%. This eliminates the error in the cumulative cuts and makes it possible that the property calculation methods use the crude property data from the correct region of the crude assay.

From the Fig.18, the yield of diesel is 13.5% calculated by AspenPlus shown in Tab. 43. In contrast, the yield of diesel is 10.7% computed by VTR method based on equidistance assumption shown in Tab. 43.

Specific gravity results are shown in Tab. 51 and Fig.21. There is an improvement in accuracy, even though the prediction errors in the original swing cut methods (Tab. 46) are already around 1%. Sulphur results show much more improvement (Tab. 52 and Fig. 22), but the swing cut methods (if they are provided with the correct yields) are still not as accurate as TBP based method.

Table 48. Hybrid model TBP prediction compared with AspenPlus

TBP		hnph TBP95	kero TBP95	dsl TBP95	kero TBP05	dsl TBP05	AGO TBP05
Aspen plus	*F*	360.0	520.0	640.0	350.0	460.0	540.0
Hybrid model	*F*	360.5	520.5	639.7	349.3	459.6	540.5
Error	*%*	0.14	0.09	-0.04	-0.21	-0.08	0.10

Table 49. Hybrid model yields prediction compared with AspenPlus

Flowrate		hnph	kero	dsl	AGO
AspenPlus	*bbl/day*	5618	16934	10707	12458
Hybrid model	*bbl/day*	5599	17145	10561	12873
AspenPlus	*LV%*	7.06	21.27	13.45	15.65
Hybrid model	*LV%*	7.03	21.54	13.27	16.17

Table 50. Product properties computed by swing cut methods

when correct yields are provided from the hybrid model

	fixed cut				VTR			L/H cut			
	Size	yield	SG	sulfur	yield	SG	Sulfur	size	yield	SG	Sulfur
	LV%	*LV%*	*g/cm3*	*wt%*	*LV%*	*g/cm3*	*wt%*	*LV%*	*LV%*	*g/cm3*	*wt%*

naphtha	3.0	7.0	0.74	0.03	7.0	0.76	0.05	3.0	7.0	0.74	0.03
sw1-l	4.0		0.79	0.23				4.0		0.79	0.18
sw1-h	1.0		0.79	0.23				1.0		0.80	0.58
kerosene	14.0	21.5	0.82	1.36	21.5	0.83	1.46	14.0	21.5	0.82	1.36
sw2-l	6.6		0.84	1.78				6.6		0.84	1.77
sw2-h	0.4		0.84	1.78				0.4		0.85	1.93
diesel	5.0	13.3	0.85	2.07	13.3	0.86	2.25	5.0	13.3	0.85	2.07
sw3-l	7.8		0.86	2.38				7.8		0.86	2.36
sw3-h	1.2		0.86	2.38				1.2		0.87	2.51
AGO	15.0	16.2	0.89	2.79	16.2	0.89	2.76	15.0	16.2	0.89	2.79

Table 51. Specific gravity prediction when using yields from the hybrid model

specific gravity	unit	nph	kero	dsl	AGO
AspenPlus	*g/cm3*	0.763	0.827	0.858	0.889
fixed cut	*g/cm3*	0.765	0.836	0.847	0.915
VTR	*g/cm3*	0.764	0.826	0.858	0.885
L/H cut	*g/cm3*	0.766	0.826	0.858	0.886
TBP cuts	*g/cm3*	0.754	0.823	0.858	0.894
fixed cut error	*%*	0.241	1.123	-1.323	2.931
VTR error	*%*	0.097	-0.064	-0.045	-0.421
L/H error	*%*	0.400	-0.082	-0.011	-0.331
TBP cut error	*%*	-1.154	-0.497	-0.033	0.515

Table 52. Sulfur prediction when using yields from the hybrid model

sulfur content	unit	hnph	kero	dsl	AGO
AspenPlus	*wt%*	0.17	1.49	2.23	2.83
fixed cut	*wt%*	0.15	1.44	2.25	2.76
VTR	*wt%*	0.05	1.46	2.25	2.76
L/H cut	*wt%*	0.12	1.45	2.24	2.77
TBP cuts	*wt%*	0.20	1.47	2.22	2.84
fixed cut error	*%*	-13.61	-3.16	0.73	-2.32
VTR error	*%*	-71.75	-1.65	0.93	-2.51
L/H error	*%*	-32.53	-2.38	0.42	-2.00
TBP cut error	*%*	18.82	-1.54	-0.92	0.01

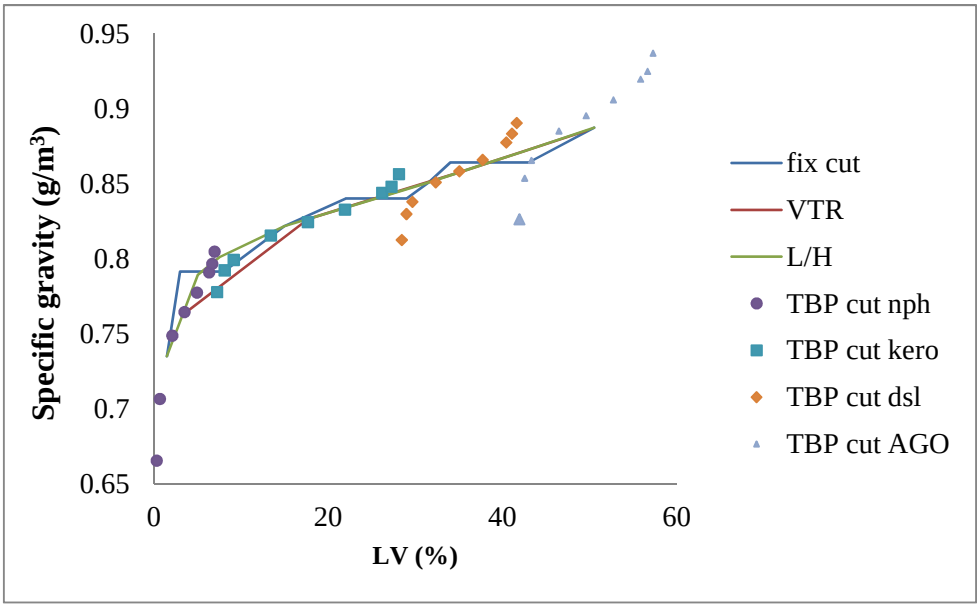

Figure 21. Specific gravity of product based on the yields from hybrid model

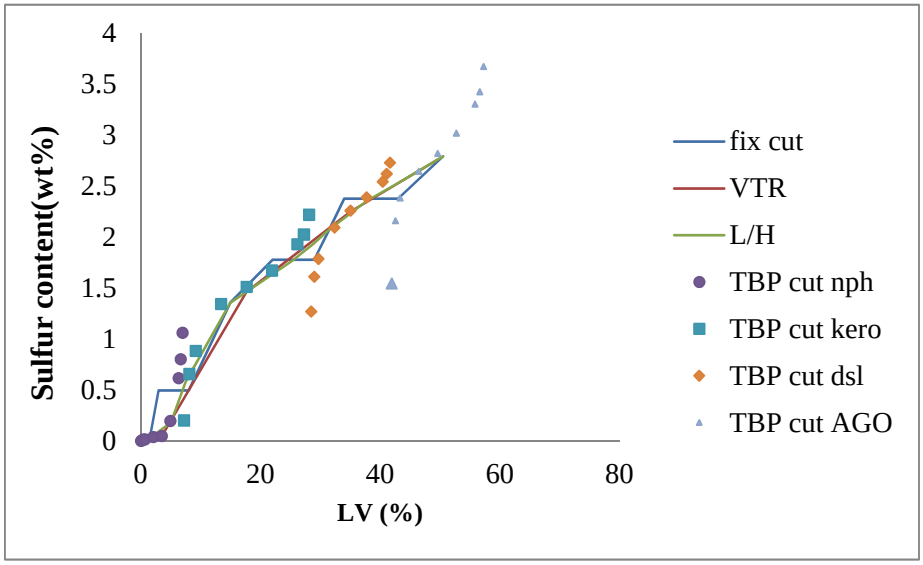

Figure 22. Sulfur content of product based on the yields from hybrid model

6. Conclusions

This work addresses the issue of inconsistency of predictions between the models which are used for planning, for scheduling, and for real time optimization of refinery operations. Over the last decade there have been many proposed versions of simplified crude distillation models. Most of these models rely on the assumption that at be boundary of the product cut the distance from the crude distillation curve to the front end of the heavier product is equal to the distance to the back end of the lighter product. In addition, many models assume that the mid-point of the product distillation curve lies on the crude distillation curve. Both of these assumptions are not correct as it can be seen from rigorous crude unit simulation or from plant data.

Hybrid model presented in this thesis removes both of these assumptions. It is a small size model of the crude unit (preflash, atmospheric, and vacuum towers) which predicts the unit behaviour with very small discrepancies (vast majority of them less than 1%) with respect to the rigorous tray to tray model. The model is linear, with exception of the reflux/(reflux+distillate) variable for the atmospheric tower. Volumetric and energy balance equations are complemented by PLS models which relate the operating variables to product distillation curves.

Extensive model testing has been carried out by comparing the model predictions with rigorous tray to tray model of the crude unit in AspenPlus. An optimization example

demonstrates that the optimum computed from the hybrid model is feasible and at least as good as the optimum computed by AspenPlus equation oriented mode.

The previous paper (Mahalec 2012) relied on the calculation of internal reflux ratios in the distillation tower. In order to calculate these ratios, one needs to know the temperatures on the corresponding trays. Such data are available in real-time operation but unavailable in production planning or scheduling. In addition, Mahalec and Sanchez modelled only the atmospheric distillation tower. The current work is wider in scope; it includes the preflash tower, the atmospheric tower, and the vacuum tower. It is a complete model of a crude distillation unit with accuracy close to the rigorous models. Moreover, this work includes properties prediction section which is not covered in the previous work by Mahalec and Sanchez (2012).

The current work presents a model which is suitable for production planning and for scheduling, in addition to RTO. Since tray temperatures for some future operation are not available in the planning or in the scheduling applications, the current model does not use internal reflux ratios. Instead, the current model uses directly the operating variables and the gap between selected TB points of the adjacent crude cuts.

Different swing cut (fixed-cut, weight/volume transfer, light/heavy) methods were compared with pseudo-cuts TBP based method which uses product TBP curves computed

via hybrid distillation model. Bulk product properties are computed by blending pseudo-cuts for each product as determined by the product TBP curves. Swing cut models use assumptions which lead to incorrect product TBP curves, resulting in lower yield accuracy. If swing cut method yields are replaced by the correct yields from hybrid model, for monotonically increasing crude properties (gravity), all four methods have the same accuracy. Non-monotonical properties (sulphur) are predicted more accurately by TBP pseudo-cuts method.

Small size of the model and excellent convergence properties make it suitable for applications in production planning, scheduling, and real-time optimization refinery applications. Therefore, this type of the hybrid models can be used to eliminate discrepancies (caused by different models) in the decisions between these business processes.

The future work will focus on integrating this hybrid model with other processing units in refinery like FCCU, Naphtha reformer etc. Then this refinery platform can be used for planning and scheduling related research.

7. References

(1). Aspen Technology Inc. Getting started: modeling petroleum processes. Cambridge, MA: Aspen Technology Inc. 2006

(2). Aspen Technology Inc. Aspen Plus 11.1 Unit Operation Models. Cambridge, MA: Aspen Technology Inc. 2001

(3). Alattas, A. M.; Grossmann, I. E.; Palou-Rivera, I. Integration of Nonlinear Crude Distillation Unit Models in Refinery Planning Optimization. Ind. Eng. Chem. Res. 2011, 50, 6860−6870.

(4). Bagajewicz M, Ji S. Rigorous procedure for the design of conventional atmospheric crude fractionation units. Part I: targeting. Ind Eng Chem Res 2001;40(2):617-626..

(5). Bagajewicz M, Soto J. Rigorous procedure for the design of conventional atmospheric crude fractionation units. Part II: heat exchanger network. Ind Eng Chem Res 2001; 40(2):627-634.

(6). Boston, J. F. and S. L. Sullivan, "A New Class of Solution Methods for Multicomponent, Multistage Processes", Can. J. Chem. Eng. 52, 52-63 (1974).

(7). Brenno C. Menezes, Jeffrey D. Kelly, and Ignacio E. Grossmann. Improved Swing-Cut Modeling for Planning and Scheduling of Oil-Refinery Distillation Units. Ind. Eng. Chem. Res.2013;52 (51):18324–18333

(8). Brooks, R. W, van Walsem, F. D.Drury, J. Choosing Cut-points to Optimize Product Yields. Hydrocarb Process.1999; 78 (11): 53−60.

(9). Chen L. Heat-integrated crude oil distillation design. PhD Thesis. Manchester,UK: University of Manchester; 2008.

(10). Fenske, M. R. Fractionation of Straight-Run Pennsylvania Gasoline.Ind. Eng. Chem. Res. 1932, 24, 482–485.

(11). Gadalla M, Olujic Z, Jobson M, Smith R. Estimation and reduction of CO2emissions from crude oil distillation units. Energy 2006; 31(13):2398e408.

(12). Geddes, R. L. A General Index of Fractional Distillation Power for Hydrocarbon Mixtures. AIChE J. 1958, 4, 389−392.

(13). Gilbert, R.; Leather, J.; Ellis, J. The Application of the Geddes Fractionation Index to The Crude Distillation Units. AIChE J. 1966,12, 432–437.

(14). Gilliland, E. R. Multicomponent Rectification: Estimation of the Number of Theoretical Plates as a Function of the Reflux Ratio. Ind. Eng.Chem. Res. 1940, 32, 1220–1223.

(15). Guerra, O. J.; Le Roux, A. C. Improvements in Petroleum Refinery Planning: 1. Formulation of Process models. Ind. Eng. Chem. Res. 2011a; 50:13403−13418.

(16). Guerra, O. J.; Le Roux, A. C. Improvements in Petroleum Refinery Planning: 2. Case studies. Ind. Eng. Chem. Res. 2011b; 50:13419−13426.

(17). J. B. Maxwell. Vapor Pressures and Latent Heats of Vaporization of Hydrocarbons.Ind. Eng. Chem.1932;24 (5): 502–505

(18). Li, W.; Hui, C.-W.; Li, A. Integrating CDU, FCC and product blending models into refinery planning. Comput. Chem. Eng. 2005;29(9): 2010–2028.

(19). Mahalec, V.; Sanchez, Y. Inferential Monitoring and Optimization of Crude Separation Units via Hybrid Models. Comput. Chem. Eng.2012; 45: 15−26.

(20). Neiro, S. M. S.; Pinto, J. M. A General Modeling Framework for the Operational Planning the Petroleum Supply Chain. Comput. Chem. Eng. 2004; 28: 871−896.

(21). Ochoa-Estopier LM, Jobson M, Smith R. The use of reduced models for design and optimisation of heat-integrated crude oil distillation systems. Energy. 2014;75:5-13.2004; 28: 871−896.

(22). Pinto, J. M.; Joly, M.; Moro, L. F. L. Planning and Scheduling Models for Refinery Operations. Comput. Chem. Eng. 2000; 24 (9−10):2259−2276.

(23). Sanchez, S.; Ancheyta, J,; McCaffrey, W.C.; Comparison of Probability Distribution Functions for Fitting Distillation Curves of Petroleum. Energy&fuels.2007,21:2955-2963

(24). Suphanit, B. The Design of Complex Distillation Systems. Ph.D.Thesis, University of Manchester Institute of Science & Technology (UMIST), Manchester, U.K., 1999.

(25). Svrcek, W, Personnal communication with Dr. Mahalec, 1989

(26). Watkins, R. N. Petroleum Refinery Distillation, 2nd ed.; Gulf Publishing Co.: Houston, TX, 1979.

(27). Zhang, J. Zhu, X. Towler, G. A Level-by-Level Debottlenecking Approach in Refinery Operation. Ind. Eng. Chem. Res. 2001;40: 1528–1540